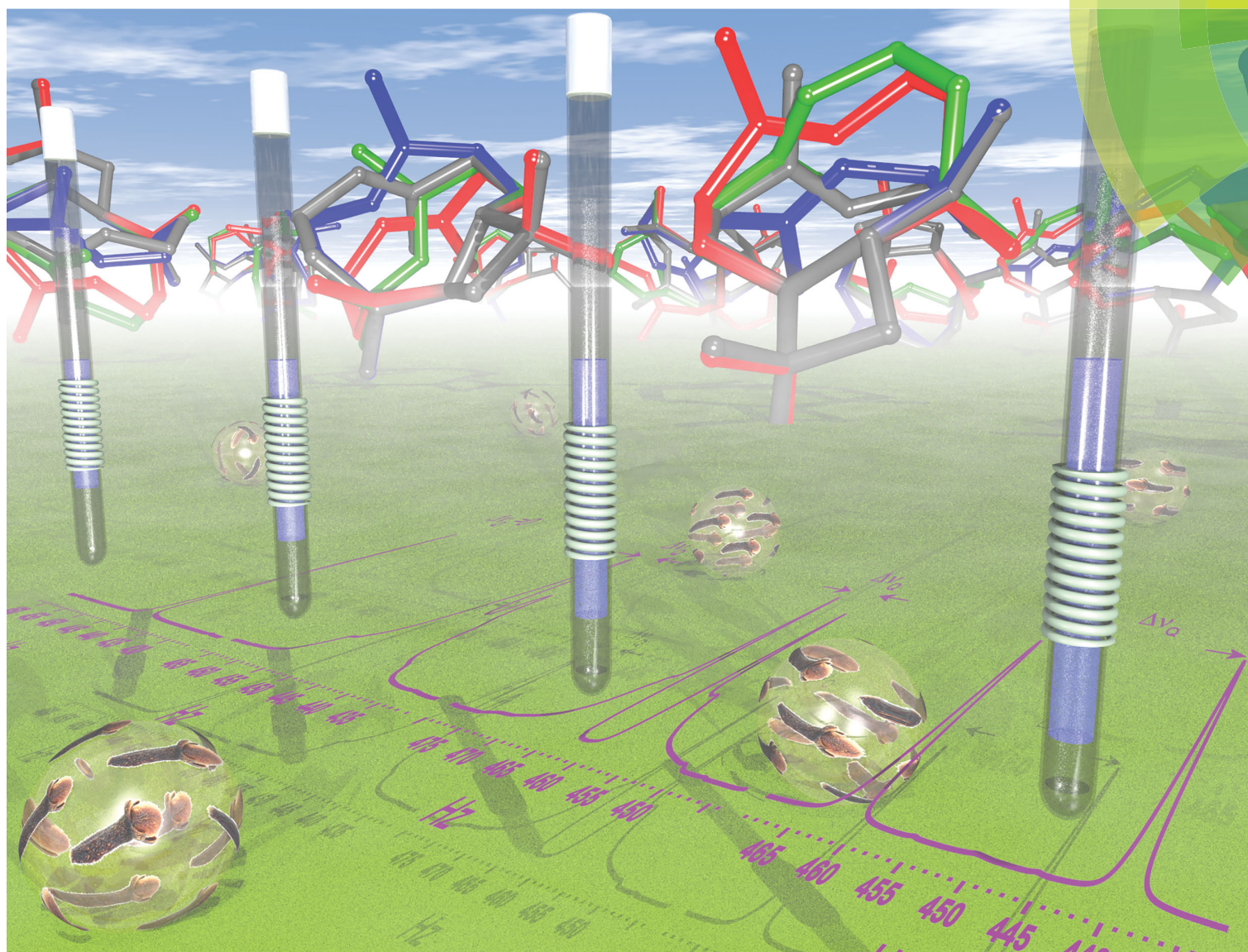
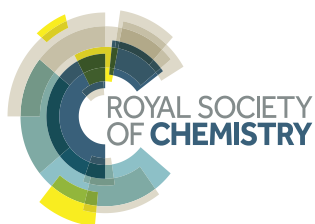


ChemComm

Chemical Communications
rsc.li/chemcomm



ISSN 1359-7345



COMMUNICATION

Christina M. Thiele *et al.*

Chemically synthesized and cross-linked PDMS as versatile alignment medium for organic compounds

COMMUNICATION



Cite this: *Chem. Commun.*, 2017, 53, 95

Received 1st November 2016
Accepted 23rd November 2016

DOI: 10.1039/c6cc08762k

www.rsc.org/chemcomm

Chemically synthesized and cross-linked PDMS as versatile alignment medium for organic compounds†

Yulia E. Moskalenko,‡§ Viktor Bagutski§ and Christina M. Thiele*

A useful procedure for the preparation of chemically synthesized and cross-linked polydimethylsiloxane (PDMS) gels is presented, which does not require β -irradiation for cross-linking. NMR spectra of high quality are obtained, such that even mixtures of compounds exhibiting similar NMR spectra like interconverting stereoisomers can be investigated in the residual dipolar coupling (RDC) approach of organic structure determination.

The determination of conformation and configuration of organic compounds usually involves the measurement of 3J couplings¹ and the nuclear Overhauser effect (NOE).² Residual dipolar couplings (RDCs) become increasingly important in the structure elucidation process due to their complementary information content.³ While 3J couplings and NOEs can be measured in isotropic solution, the compound in question needs to be oriented with respect to the magnetic field to get access to RDCs. Anisotropy in the orientation of the compound is induced *via* suitable alignment media, which should be compatible with organic solvents and solutes, should be homogeneous and ideally also scalable. For organic compounds there are two main classes of alignment media: namely lyotropic liquid crystals and anisotropically swollen cross-linked polymer gels.³ The former have the advantage of a quick sample preparation; scalability, however, is limited.^{4,5} For the latter it is known that a scaling of the order induced in the compound can be performed either *via* different cross-linking degrees (before sample preparation)⁶ or even on the readily prepared gel using a gel-stretching device.^{7,8} Swelling of gels in the NMR sample tube can be a time-consuming

process, though. A series of cross-linked polymer gels already exist. Apart from poly(methyl methacrylate) (PMMA) gels, from which initiators and cross-linkers can be removed *via* reversible compression and release,⁸ and thermally cross-linked polystyrene⁹, polymer gels normally contain some impurities due to their fabrication process (residual monomer, radical initiator, cross-linker). These can lead to solute incompatibilities or residual signals in the NMR spectrum. In this respect PDMS gels stand out as they have so far been made by irradiation with β -rays.¹⁰ Furthermore, the residual signal of PDMS appears in a region in the spectrum (around 0 ppm in ^1H , ^{13}C and ^{29}Si) where it does not overlap with signals of commonly studied compounds.

In this communication, we present a procedure for the preparation of PDMS sticks requiring neither β -irradiation nor radical initiators during polymerisation and/or cross-linking. It is shown that the gels obtained are suitable as alignment medium even for sensitive compounds. High-quality NMR spectra are obtained, which allow investigating mixtures of compounds exhibiting similar NMR spectra such as stereoisomers.

The beauty of the synthetic procedure (see Scheme 1) lies in the use of one single starting material octamethylcyclotetrasiloxane (D_4) for polymer, initiator and cross-linker.^{11,12}

Thus no non-silicone cross-linkers are used alleviating problems of unwanted rearrangements as well as parasitic signals of compounds related to the manufacturing process of the gel. The PDMS gel with living anionic ends would allow for exploitation of self-healing properties,¹¹ which can in principle be used for direct preparation of the gel inside the NMR sample tube. This has not been exploited here, though.

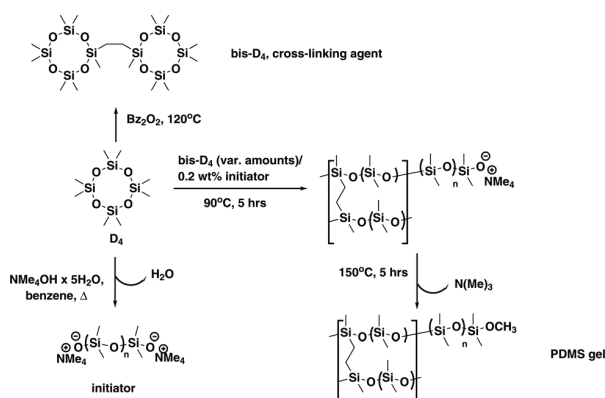
An annealing step at 150 °C is used to “decatalyse” the living polymer (removal of NMe_3),^{11,13} making the polymer gel stable and thus suitable for its use as alignment medium. While dibenzoyl peroxide (Bz_2O_2) is used in the preparation of the cross-linking agent bis(heptamethylcyclotetrasiloxanyl)-ethane (bis- D_4), this can be removed by various purification steps (see ESI†) before the actual gel is produced. We envisaged that using this living anionic polymerisation would allow for the preparation of a homogeneous and contamination-free alignment medium

Clemens-Schöpf-Institut für Organische Chemie und Biochemie, Technische Universität Darmstadt, Alarich-Weiss-Strasse 16, 64287 Darmstadt, Germany.
E-mail: cthiele@thielelab.de

† Electronic supplementary information (ESI) available: Detailed synthesis procedure for PDMS sticks, RDC data on β -(-)-caryophyllene and IPC, investigation of PDMS decomposition, theory to predict quadrupolar splittings induced, representative spectra in PDMS gels. See DOI: 10.1039/c6cc08762k

‡ Current address: Instituto de Química, Universidade de São Paulo, Av. Prof. Lineu Prestes, 748, 05508-900 São Paulo-SP, Brazil.

§ These authors have contributed equally to this work.



Scheme 1 Synthetic procedure for the preparation of PDMS gels: starting from octamethylcyclotetrasiloxane (D_4), the cross-linking agent bis(heptamethylcyclotetrasiloxanyl)-ethane (bis- D_4) as well as the initiator bis(tetramethylammonium)oligodimethylsiloxanediolate are prepared.

with improved spatial regularity ensured by the essentially equilibrative character of the polymerisation process.

For the preparation of the gels an array of molds easily prepared from commercially available PTFE tubing (3 or 3.2 mm inner diameter) was filled with degassed polymerising mixture of varying cross-linker content and subjected to polymerisation at 90 °C (see ESI†) over 5 h to afford the PDMS-sticks of an appropriate quality after thermal decatalysing† (see Scheme 1). The sticks obtained *via* this procedure were introduced into NMR tubes and swollen in $CDCl_3$. Quadrupolar deuterium splitting $\Delta\nu_Q$ of $CDCl_3$ is taken as indicator of anisotropy.

The swelling process of the gel sample over time and the assessment of its homogeneity can conveniently be performed by 2H imaging¹⁴, a technique that allows for obtaining 2H spectra as a function of z -position (see Fig. 1).

As solvent is added to the top and to the bottom of the NMR tube in the sample preparation process (see ESI†), these regions display the largest quadrupolar splittings in the beginning (see Fig. 1a and d) indicating the largest degrees of swelling. Within one week (see Fig. 1c and f) samples reach sufficient axial homogeneity for RDC investigations. Only a slight increase of

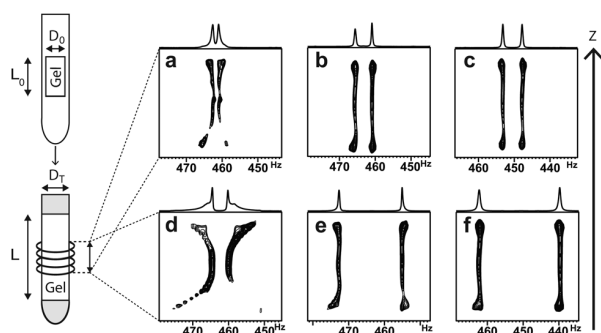


Fig. 1 2H NMR images of PDMS gels at 300 K after swelling in $CDCl_3$ (5 mm OD NMR tubes) over 18 h (a and d), 4 days (b and e) and 8 days (c and f). Gels contained 0.5 mol% of bis- D_4 (top row: a–c) and 1.3 mol% of bis- D_4 (bottom row: d–f).

Table 1 Initial and final parameters of PDMS sticks swollen in $CDCl_3$ inside an NMR tube at 300 K. bis- D_4 denotes the content of cross-linker; L_0 , D_0 are the length and diameter of the unswollen polymer stick, L_{eq} and D_{eq} the length and diameter of the equilibrated polymer gel

bis- D_4 /mol%	L_0 /mm	L_{eq} /mm	D_0 /mm	D_{eq} /mm	$\Delta\nu_Q$ /Hz
0.5	14	52	3.0	4.09	6.8
1.0	14	41	3.0	4.09	22.7
1.3 ^a	14	35	3.0	4.09	23.2
1.5	14	35	3.2	4.20	47.6
2.0	14	35	3.2	4.20	42.8

^a 1.35 mol% of initiator used; this could be responsible for the small $\Delta\nu_Q$.

$\Delta\nu_Q$ (<5% per day) is observed afterwards indicating an asymptotical behaviour of swelling near the saturation point. The fully equilibrated gels exhibit $\Delta\nu_Q$ in a range between 7 and 48 Hz as it is shown in Table 1. As can be seen from the values in Table 1 and is known for other gels^{6,15} the degree of swelling can be influenced by the choice of the diameters of the mold, the inner diameter of the NMR tube (entries 1–3 vs. 4 and 5) and the cross-linker density. Here, beyond 2 mol% of cross-linker no increase in splitting is observed anymore.

While we did not do the detailed investigation here, it is to be expected that the different quadrupolar splittings of the solvent translate into different degrees of orientation and thus into different sizes of RDCs for the solutes to be investigated.

A clear advantage of our gel preparation protocol is that the parameters required for the characterization of the physical state of the gels are well known, allowing for the modeling of $\Delta\nu_Q$, the measured quadrupolar splitting of the gel solvent. As further discussed in the theory section of ESI† one has $\Delta\nu_Q = \Delta\nu_Q^0 \varepsilon \phi S$, where S is the order parameter for monomer orientations, ϕ is the chain monomer volume fraction and $\Delta\nu_Q^0 = 168$ kHz¹⁶ is the quadrupolar splitting of perfectly aligned $CDCl_3$ molecules. The efficiency factor ε accounts for the transfer of orientation between the partially oriented chain monomers and the solvent molecules during a solvent–monomer encounter; it is an intrinsic property of each given solvent–monomer pair. The careful measurement of gel and tube dimensions at all stages of our experiments and the knowledge of the cross-linking molar ratios allows computing ϕ and S from standard polymer-gel theory. We found (see ESI†) good agreement between theory and experiments and determine the efficiency for this particular gel–solvent pair $\varepsilon = 6.5 \pm 0.5 \times 10^{-3}$, roughly at one part per 150. This in turn provides for the quantitative prediction of $\Delta\nu_Q$ values for any tube stretching experiments performed for the polymer/solvent pair PDMS/ $CDCl_3$. Predictions for other polymer solvent systems would simply require performing similar sets of experiments to extract the corresponding orientation efficiency factors ε . We believe that this will allow for the tailor-made synthesis of PDMS-sticks in the future.

To highlight the suitability of the synthesized PDMS gel for the acquisition of high quality RDC data sets we have chosen the ubiquitous natural sesquiterpene β (–)-caryophyllene (BCP). It is deemed a challenging object for structure elucidation due to its known complex conformational composition exhibiting more than one signal set (Fig. 2).¹⁷

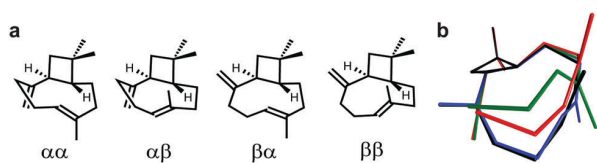


Fig. 2 (a) β -(-)-Caryophyllene conformers (descriptors convention: α – “down”, β – “up”, first: methylene group, second: alkenyl-CH₃) and (b) their cumulative 3D representation ($\alpha\alpha$ – green, $\alpha\beta$ – red, $\beta\alpha$ – blue and $\beta\beta$ – black). Putative conformer $\alpha\beta$ is not present in the mixture as it is energetically disfavoured.¹⁷

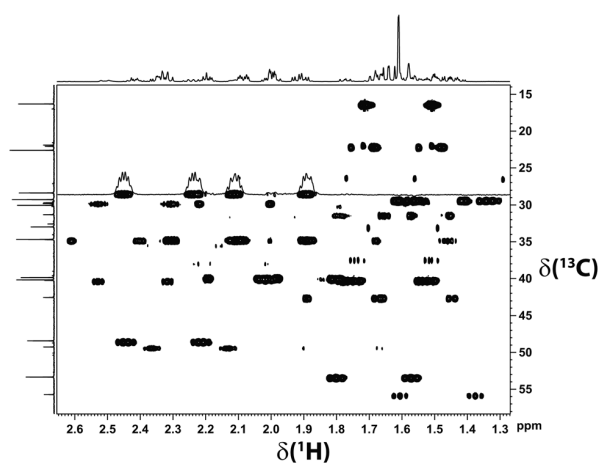


Fig. 3 Section of the CLIP-HSQC spectrum¹⁸ of β -(-)-caryophyllene recorded in a chemically synthesized PDMS gel equilibrated in CDCl₃. The high quality of the spectrum allows for the precise extraction of $^1D_{C-H}$. Note that two signal sets of different proportion are visible. The quality of the acquired data is very high; even the fine structure of the multiplets is visible.

The composition of the solution equilibrium of conformations has been determined NMR-spectroscopically at low temperature (120 K) previously,¹⁷ but no assignment of diastereotopic protons has been published so far. Thus BCP is the ideal candidate to demonstrate the suitability of chemically synthesized PDMS gel for the analysis of complex mixtures.

For the RDC measurements we thus equilibrated a PDMS gel with 1.3 mol% cross-linker density in a BCP/CDCl₃ (5 μ L mL⁻¹) solution. The spectra were of excellent quality (see Fig. 3).

As can be seen in Fig. 3, two signal sets – one of higher and one of lower intensity – are obtained. At low temperatures the minor signal set corresponds to the $\beta\beta$ -conformer, whereas the remaining signal set was assigned to interconverting $\alpha\alpha$ - and $\beta\alpha$ -conformers.¹⁷

Accordingly, two sets of RDCs were obtained for the two signal sets; values varied between -1 and $+4$ Hz at 279 K (using the $J + 2D$ convention for T) (see ESI[†]). Thus we fitted the RDCs belonging to the signal set of lower intensity to the DFT calculated geometry of the $\beta\beta$ -conformer using our in-house developed software RDC@hotfcht.^{19,20} As can be seen in Fig. 4a an excellent fit of RDCs of the minor signal set to the coordinates of the $\beta\beta$ -conformer was obtained. Fitting of these data to the (DFT derived) coordinates of the $\alpha\alpha$ - or $\beta\alpha$ -conformers

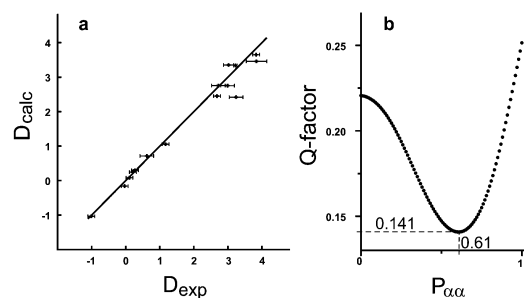


Fig. 4 (a) Correlation plot of 15 RDCs measured for the minor signal set to the coordinates of the $\beta\beta$ -conformer of BCP ($Q = 0.074$); (b) population scan (1% steps) for the 17 RDCs of the major signal set to the coordinates of the $\alpha\alpha$ - and $\beta\alpha$ -conformers. The population with the best agreement with experimental data is $P_{\alpha\alpha} = 0.61$ ($Q = 0.141$).

yielded a significantly poorer agreement (as indicated by a larger Q -factor) (see ESI[†]) confirming the assignment of the minor signal set to the $\beta\beta$ -conformer.

For the major signal set 17 RDCs were obtained. As it is expected that this signal set does not belong to a single conformer, but is due to interconverting conformers, flexibility needs to be taken into account in the fitting procedure.²⁰ Fitting the RDCs in a multi-conformer single-tensor analysis to the coordinates of the $\alpha\alpha$ - and $\beta\alpha$ -conformer (1% step size in the population scan) leads to an excellent agreement with experimental data at $\alpha\alpha:\beta\alpha = 61:39$ (see Fig. 4b). Thus this composition is assumed to be the one present in solution (in the anisotropic sample at 279 K). This outcome turns out to be in excellent agreement with the previously published results of both – an experimental (63% of $\alpha\alpha$ at 120 K)¹⁷ and a computational study (67.8% of $\alpha\alpha$)²¹. Additionally, we provide the so far missing diastereotopic assignment of all protons (see ESI[†]).

In terms of its practical application as alignment medium it is important to note that PDMS is not limited to CDCl₃ as solvent, but also swells in THF^{10,22} and even at lower temperatures (253 K was chosen here). As might be expected, swelling time is increased with decreasing temperature (see ESI[†]).

The applicability at lower temperatures greatly extends the scope towards covering air- and heat-sensitive (non-basic, see below) organometallic compounds. We have used this feature in the investigation of structure and dynamics of η^1 -coordinated Pd-intermediates.²² As can be seen in Fig. 5 the spectral quality is excellent despite the two species A and B being present simultaneously.

Thus chemically synthesized PDMS is a versatile alignment medium, which owing to the excellent spectral quality allows for investigating mixtures of rather similar compounds. An application to the structural analysis of a peptide will be presented separately.²³

It is worth mentioning here that in terms of solute and solvent compatibility the inherent sensitivity of PDMS towards Brønsted bases needs to be taken into account.²⁴ Contrary to our expectation neither the Pd-complexes described above nor the trimethylamine liberated in the decatalysing step cause any problems in anhydrous solvents. In a wet solvent, however, slow

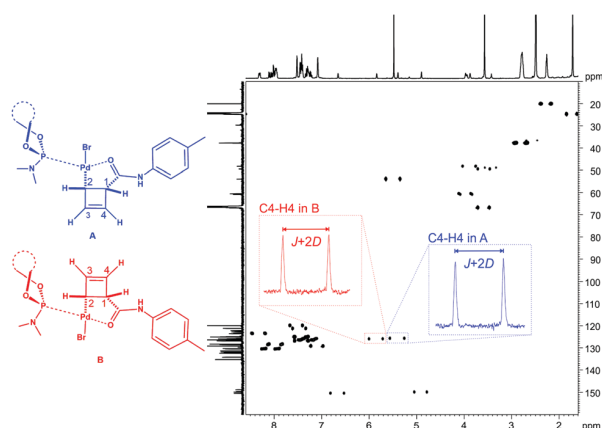


Fig. 5 CLIP-HSQC spectrum¹⁸ of diastereomeric Pd-complexes A and B²² in chemically cross-linked PDMS (1.25 mol% cross-linker density) swollen in THF-*d*₆ (swelling performed at 253 K, measurement performed at 293 K). The phosphoramidite ligand indicated is MonoPhosTM.

decomposition of the PDMS-gel may happen. Slow decomposition was also observed in the case of an attempted RDC measurements of (+)-isopinocampheol (IPC) in chloroform (see ESI[†]). Interestingly, the same tendency for decomposition in the presence of (+)-IPC has been also displayed by a sample of PDMS produced by β -irradiation (gift from the Luy group). Thus this incompatibility is not a result from the synthetic procedure.

On a positive side, this feature can readily be exploited to develop a facile procedure for the removal of used PDMS from the NMR tubes. It was found that the simple addition of THF slightly basified with a few drops of methanolic NaOH completely liquefies the gel. This allows for the easy recovery of the expensive “Young’s” NMR-tubes, which are a prerequisite for NMR measurements of highly air- and moisture sensitive compounds.

In this communication, we have presented a valuable procedure for the chemical synthesis of PDMS gels for the use as alignment medium in NMR-spectroscopy. The high regularity obtained by the synthetic procedure enables the acquisition of spectra of excellent quality, such that even mixtures of compounds exhibiting similar NMR spectra can be investigated. This is exemplified here for the sesquiterpene β -(-)-caryophyllene (BCP) and for a mixture of η^1 -coordinated Pd-intermediates. The known incompatibility of PDMS with Brønsted bases is exploited for introducing a cleaning procedure for expensive NMR tubes.

Furthermore, the known cross-linker content and careful monitoring of the swelling geometry allowed for the successful comparison between polymer gel theory and experiments, providing the calibration of the orientation efficiency factor for the PDMS/ CDCl_3 pair, which will enable the preparation of PDMS gel sticks with predefined orientational order.

The authors thank Burkhard Luy for providing PDMS sticks obtained by β -irradiation and for helpful discussions concerning

soluble compatibility. We thank Dr C. M. Marques (ICS CNRS, Stasbourg) for his help with the evaluation of gel anisotropy and prediction of solvent quadrupolar splittings. PD Dr S. Immel and Dr V. Schmidts provided help with the DFT calculations of the BCP conformers. This work was supported by the ERC (St. G. 257041 to C. M. T.).

Notes and references

† The polymerization process was terminated by heating at 150 °C for 5 h to accomplish thermal decomposition of the catalyst liberating a minuscule amount of trimethylamine.

- C. A. G. Haasnoot, F. A. A. M. de Leeuw and C. Altona, *Tetrahedron*, 1980, **36**, 2783–2792.
- F. A. L. Anet and A. J. R. Bourn, *J. Am. Chem. Soc.*, 1965, **87**, 5250–5251; C. P. Butts, C. R. Jones and J. N. Harvey, *Chem. Commun.*, 2011, **47**, 1193–1195.
- Reviews: C. M. Thiele, *Eur. J. Org. Chem.*, 2008, 5673–5685; G. Kummerlöwe and B. Luy, *Trends Anal. Chem.*, 2009, **28**, 483–493; R. R. Gil, *Angew. Chem., Int. Ed.*, 2011, **50**, 7222–7224; V. Schmidts, *Magn. Reson. Chem.*, 2016, DOI: 10.1002/mrc.4543.
- A. Marx and C. Thiele, *Chem. – Eur. J.*, 2009, **15**, 254–260.
- C. M. Thiele, *Angew. Chem., Int. Ed.*, 2005, **44**, 2787–2790.
- B. Luy, K. Kobzar and H. Kessler, *Angew. Chem., Int. Ed.*, 2004, **43**, 1092–1094; B. Luy, K. Kobzar, S. Knör, J. Furrer, D. Heckmann and H. Kessler, *J. Am. Chem. Soc.*, 2005, **127**, 6459–6465; R. R. Gil, C. Gayathri, N. V. Tsarevsky and K. Matyjaszewski, *J. Org. Chem.*, 2008, **73**, 840–848.
- R. Tycko, F. J. Blanco and Y. Ishii, *J. Am. Chem. Soc.*, 2000, **122**, 9340–9341; P. W. Kuchel, B. E. Chapman, N. Müller, W. A. Bubb, D. J. Philp and A. M. Torres, *J. Magn. Reson.*, 2006, **180**, 256–265; G. Kummerlöwe, F. Halbach, B. Laufer and B. Luy, *Open Spectrosc. J.*, 2008, **2**, 29–33.
- C. Gayathri, N. V. Tsarevsky and R. R. Gil, *Chem. – Eur. J.*, 2010, **16**, 3622–3626.
- A.-C. Pöppler, H. Keil, D. Stalke and M. John, *Angew. Chem., Int. Ed.*, 2012, **51**, 7843–7846.
- J. C. Freudenberger, P. Spittler, R. Bauer, H. Kessler and B. Luy, *J. Am. Chem. Soc.*, 2004, **126**, 14690–14691.
- P. Zheng and T. J. McCarthy, *J. Am. Chem. Soc.*, 2012, **134**, 2024–2027.
- O. K. Johansson, *US Pat.*, 2762827, 1956; S. W. Kantor, *US Pat.*, 2785147, 1957; S. W. Kantor and R. C. Ostoff, *US Pat.*, 2793222, 1957.
- A. R. Gilbert and S. W. Kantor, *J. Polym. Sci.*, 1959, **11**, 35–58.
- P. Trigo-Mouriño, C. Merle, M. R. M. Koos, B. Luy and R. R. Gil, *Chem. – Eur. J.*, 2013, **19**, 7013–7019.
- T. Montag and C. M. Thiele, *Chem. – Eur. J.*, 2013, **19**, 2271–2274.
- B. Deloche, A. Dubault and D. Durand, *J. Polym. Sci., Part B: Polym. Phys.*, 1992, **30**, 1419–1421.
- M. Hübner, B. Rissom and L. Fitjer, *Helv. Chim. Acta*, 1997, **80**, 1972–1982.
- A. Enthart, J. C. Freudenberger, J. Furrer, H. Kessler and B. Luy, *J. Magn. Reson.*, 2008, **192**, 314–322.
- V. Schmidts, PhD thesis, Technische Universität Darmstadt, 2013; R. Berger, C. Fischer and M. Klessinger, *J. Phys. Chem. A*, 1998, **102**, 7157–7167.
- C. M. Thiele, V. Schmidts, B. Böttcher, I. Louzao, R. Berger, A. Maliniak and B. Stevansson, *Angew. Chem., Int. Ed.*, 2009, **48**, 6708–6712.
- M. Clericuzio, G. Alagona, C. Ghio and L. Toma, *J. Org. Chem.*, 2000, **65**, 6910–6916.
- L.-G. Xie, V. Bagutski, D. Audisio, L. M. Wolf, V. Schmidts, K. Hoffmann, C. Wirtz, W. Thiel, C. M. Thiele and N. Maulide, *Chem. Sci.*, 2015, **6**, 5734–5739.
- M. Fredersdorf, M. Kurz, A. Bauer, M. O. Ebert, C. Rigling, L. Lannes and C. M. Thiele, manuscript in preparation.
- J. N. Lee, C. Park and G. M. Whitesides, *Anal. Chem.*, 2003, **75**, 6544–6554.

Electronic Supporting Information

Chemically cross-linked PDMS as versatile alignment medium for organic compounds

Yulia E. Moskalenko, Viktor Bagutski, Christina M. Thiele

Technische Universität Darmstadt, Clemens Schöpf Institut für Organische Chemie und
Biochemie, Alarich-Weiss-Str. 16, 64287 Darmstadt, Germany

Contents

Materials and Methods	S3
General	S3
NMR experiments	S3
Preparation of PDMS-sticks.....	S4
1. Cross-linker (Bis-D ₄)	S4
2. Polymerization Catalyst	S4
3. Polymerization	S5
Data for swelling of PDMS sticks in THF- <i>d</i> ₈	S6
RDC structure elucidation for β -(-)-cariophyllene (BCP) in 2.6% PDMS gel	S7
NMR spectral assignment (CDCl ₃ at 279 K) and RDC data	S7
Cartesian coordinates for the three conformers	S10
RDC cross-fits:.....	S13
$\beta\beta$ -BCP RDCs fitted to Cartesian coordinates of either $\alpha\alpha$ conformer or $\beta\alpha$ conformer	S13
Anisotropic alignment study of (+)-isopinocampheol and its acetyl ester	S14
Interaction of PDMS with IPC	S15
(+)-Isopinocampheol acetate	S15
RDC structure elucidation for (+)IPC-OAc	S16
NMR Studies of PDMS-decomposition.....	S17
²⁹ Si NMR spectroscopy of PDMS and oligodimethylsiloxanes	S17
DOSY-study of PDMS-decomposition	S18
Predicting solvent quadrupolar splitting in a swollen gel	S19
NMR spectra	S26
References and Notes.....	S38

Materials and Methods

General. All reagents were used as received from commercial suppliers unless otherwise stated. Reaction progress was monitored by thin layer chromatography (TLC) performed on Macherey Nagel aluminum plates coated with silica gel containing green fluorescence indicator for short wave UV (254nm). Visualization was achieved by UV light (254 nm), saturated aqueous potassium permanganate or 5% ethanolic solution of phosphomolybdic acid and subsequent heating.

NMR experiments. All NMR experiments were obtained on Bruker DRX-400, Avance-III HD-400 and Avance-III-600 spectrometers. Chemical shifts (δ) are referenced from TMS (0 ppm in ^1H , ^{13}C and ^{29}Si NMR) or residual CDCl_3 signal (7.27 ppm in ^1H NMR and 77.3 in ^{13}C NMR spectra). Assignment of NMR spectra of (+)-isopinocampheol and β -(-)-cariophyllene was performed using standard 1D- and 2D-NMR techniques (including H2BC)^[1]. Diastereotopic protons of β -(-)-cariophyllene were assigned using ^3J -couplings analysis obtained from DQF-COSY experiment. The PDMS was analyzed using 1D and 2D ^{29}Si NMR (1D-inept, 1D-ig, ^1H - ^{29}Si HMBC). Decomposition of PDMS in the presence of (+)-isopinocampheol was investigated by ^1H DOSY experiment (stimulated echo with bipolar gradients, Bruker pulse sequence library *stebppg1s*)^[2] performed on Avance-III HD-400 NMR spectrometer equipped with either 5 mm inverse probe with Z-gradient or 5 mm microimaging probe equipped with Diff30L Z-gradient with lock channel and 60 A GREAT amplifier. The RDC data ($D_{\text{C-H}}$) were extracted from CLIP-HSQC,^[3] scaled F_1 -coupled BIRD-HSQC^[4] and scaled F_1 -coupled BIRD-HSQC spectra with MQ-evolution^[5]. These were recorded for isotropic and anisotropic samples and RDCs are calculated according to the formula:

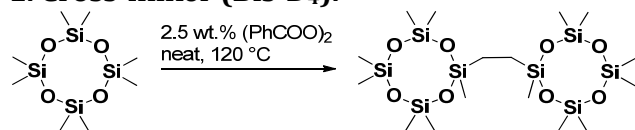
$$^1D_{\text{C-H}} = (^1T_{\text{C-H}}^{\text{aniso}} - ^1J_{\text{C-H}}^{\text{iso}}) / 2$$

For the methyl groups the $D_{\text{C-C}}$ rather than $D_{\text{C-H}}$ was used for the spatial structure elucidation. The following equation was applied ^[6]:

$$^1D_{\text{CC}} = ^1D_{\text{CH}_3} (-3\gamma_{\text{C}} / \gamma_{\text{H}}) (r_{\text{CH}}^3 / r_{\text{CC}}^3)$$

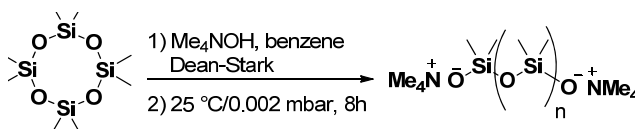
Preparation of PDMS-sticks.

1. Cross-linker (Bis-D₄).



To moderately stirred neat octamethyltetrasiloxane [D₄ (17.3 g)] at 120 °C freshly recrystallized (ethanol-water) dry benzoyl peroxide (450 mg) was gradually added (CAUTION! avoid an addition of big chunks/portions; in total it may take about 1 h; the smoother the addition is, the higher is the yield). After completion, the reaction mixture was heated for an additional 30 min, cooled to room temperature and passed through a plug of activated alumina (2.5×3 cm) and washed with petrol ether. After removing of solvents under reduced pressure, D₄ was recovered by distillation in a vacuum of water-jet pump (b.p. 62–64°C/~10 Torr). The residue was purified by multiple Kugelrohr distillations collecting a middle fraction boiling between 100–120 °C/0.01 mbar until the product is free of aromatic contaminations and crystallizes as colorless needles (m.p. 55 °C). Yield: 353 mg. ¹H NMR (600 MHz, CDCl₃, 300 K) δ = 0.47 (s, 2 H, CH₂), 0.1–0.08 (m, 18 H, 6 CH₃), 0.08 (s, 3 H, CH₃) ppm. ¹³C NMR (150 MHz, CDCl₃, 300 K) δ = 8.2 (2 CH₂), 0.8 (6 CH₃), -1.6 (CH₃) ppm. ²⁹Si NMR (119.3MHz, CDCl₃, 300 K) δ = -19.15, -19.24, -19.37 ppm.

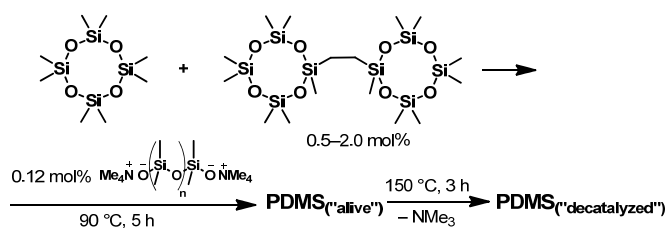
2. Polymerization Catalyst.



A mixture of 3.3 mL (11 mmol, 1.1 equivalents) of D₄ and tetramethylammonium hydroxide pentahydrate (1.8 g, 10 mmol) was refluxed in benzene (60 mL) with Dean-Stark trap until the water doesn't separated any more (typically overnight). At this point, the solution should be completely homogeneous. Then, the majority of benzene was distilled off at atmospheric pressure and the rest of volatile material was removed in high vacuum to result in a colorless waxy semisolid. It was transferred in a glove-box and used there without additional purification. The purity is estimated to be ~75% from its crude ¹H NMR spectra.

¹H NMR (400 MHz, CDCl₃, 300 K) δ = 2.79 (s, 24 H, 2 NMe₄), 0.44 (s, 12 H, 4 CH₃), 0.36 (s, 24 H, 8 CH₃) ppm.

3. Polymerization.



A 5-mL round-bottom flask was weighed in a glove-box and a little crumble of the polymerisation catalyst (see above) was stuck to the internal surface of the flask with spatula tip. A PTFE-coated stirring bar followed, the flask was closed with a septum and removed from the glove-box. 4 wt%-stock solution (4 wt%=2mol %) of bis-D₄ in D₄ was diluted with D₄ to reach the required cross-linker concentration (see above 0.5-2 mol%) and added by stirring to the polymerisation catalyst in such amount to adjust the catalysts concentration exactly to 0.12 mol %. After complete homogenization (about 30 min; don't wait any longer if you see it's dissolved, otherwise it might become too viscous for subsequent sampling with the syringe), the polymerizing mixture was withdrawn with syringe and evenly distributed within the array of semi-closed pieces of PTFE tube (ID 3 or 3.2 mm, l~25-30 mm) packed in the Schlenk tube under argon. The Schlenk was carefully (CAUTION! DO IT SLOWLY!) evacuated, purged with argon and placed in an oven pre-heated to 90 °C. To equalize the pressure in the reaction flask one can pierce the septum with a thin needle, or, more correctly, use any kind of "CaCl₂-tube" packed with activated molecular sieves. After the time required (typically, 5 h), the temperature was raised to 150 °C and polymerization was terminated (decatalysed, removal of NMe₃) by heating for at least 3 h. Then, the reaction vessel was cooled to room temperature under argon, the tipped ends of the PTFE-tubes were cut with a razor blade and thus prepared PDMS-sticks were pushed out by 2.5-3 mm rod. To protect the surface of the stick, a piece of finger-rolled cotton was placed between rod and stick. The freshly prepared PDMS sticks were dried at ambient temperature *in vacuo* (0.002 mbar) over night.

Data for swelling of PDMS sticks in THF-*d*₈.

1.2 mol% bis-D₄ in THF-*d*₈, at 300K. Start: 10/04/2013, 15:00.

<i>time</i> , h	42h 12/04, 9:23	+72h 15/04, 9:24	+2h 15/04, 11:34	+6h 15/04 17:56	+18h 16/04 12:08	+23h 17/04, 11:02	+47h 19/04 9:53
$\Delta\nu_Q$, Hz	4.4/3.6	7.0/5.6	7.1/5.7	7.2/5.8	7.5/5.9	7.8/6.2	8.1/6.4

Swelling has been performed at room temperature, measurement performed at 300K at an Avance-III-600 spectrometer.

1.5 mol% bis-D₄ in THF-*d*₈, at 263K. Start: 23/05/2013, 18:00.

<i>time</i> , h	161h 30/05, 11:20	+25h 31/05, 12:27	+26h 01/06, 14:27	+34h 03/06, 00:48	+8h 03/06, 9:05
$\Delta\nu_Q$, Hz	6.0/4.5	6.5/4.9	6.8/5.2	7.1/5.4	7.2/5.4

Swelling has been performed at 253K, measurement performed at 263K at an Avance-III-600 spectrometer.

RDC structure elucidation for β -(-)-cariophyllene (BCP) in PDMS gel

NMR spectral assignment (CDCl_3 at 279 K) and RDC data

Previously, NMR experimental data^[7] in $\text{Me}_2\text{O}-d_6$ or DFT calculated chemical shifts^[8] were published. Here we provide the full NMR attribution of BCP in CDCl_3 , including assignment of diastereotopic protons. For the spatial structure representation one can use the Cartesian coordinates for the three naturally populated conformers provided here below.

For the isotropic sample 50 μL of BCP was dissolved in 0.5 mL of CDCl_3 . Anisotropic measurements were performed for a PDMS gel sample containing 1.3 mol% of cross-linker and solution of 5 μL of BCP in 1 mL of CDCl_3 . About half of the BCP solution was placed at the bottom of an 5 mm OD NMR tube, then a PDMS stick (length 14 mm) was pushed inside using a rod such that the gel would be in the coil of NMR spectrometer. The rest of BCP/ CDCl_3 solution was added to the top of the PDMS stick (the stick floats in CDCl_3 and needs to be hold covered by the solution by putting a rod on the top of the stick until the stick swells – usually a matter of 1-2 minutes). The anisotropic gel was then equilibrated at 279 K. All NMR measurements for both isotropic and anisotropic samples were performed at 279 K on Avance-III-600 spectrometer.

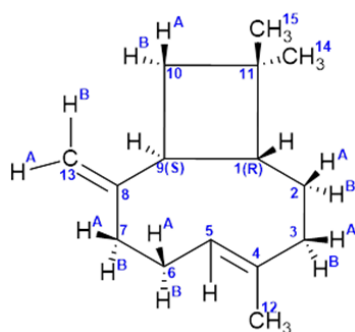


Table SI-1. Assignment and RDCs for $\alpha/\beta\alpha$ conformers (isochronous NMR signals) of BCP.

NMR attribution			
C	δ_C , ppm	H	δ_H , ppm
C1	53.3	H1	1.68
C2	29.3	H2A	1.51
		H2B	1.44
C3	39.9	H3A	1.91
		H3B	2.08
C4	135.6	-	-
C5	124.2	H5	5.31
C6	28.4	H6A	1.99
		H6B	2.34
C7	34.7	H7A	2.00
		H7B	2.20
C8	154.6	-	-
C9	48.4	H9	2.32
C10	40.2	H10A	1.65
		H10B	1.65
C12	16.3	H12	1.61
C11	33.0	-	-
C13	111.7	H13A	4.82
		H13B	4.94
C14	22.6	H14	0.97
C15	30.0	H15	1.00

Coupling nuclei		$^1D_{\text{exp}}$, Hz	
		CLIP HSQC	F_1 -cpd HSQC (MQ evol.)
C1	H1	3.37±0.10	3.38±0.30
C2	H2A	-0.50±0.30	no
	H2B	3.63±0.20	no
H2A	H2B	-	4.50±0.20
C3	H3A	3.80±0.20	4.04±0.20
C3	H3B	-0.04±0.10	-0.02±0.50
C5	H5	2.91±0.10	2.96±0.10
C6	H6A	1.79±0.30	2.08±0.20
	H6B	0.18±0.30	0.33±0.20
H6A	H6B	-	5.90±0.20
C7	H7A	1.45±0.50	1.86±0.20
C7	H7B	-0.01±0.30	-0.18±0.80
C9	H9	3.61±0.10	3.66±0.10
C10	H10A	Str. Coupl.	8.47±0.10
	H10B	Str. Coupl.	-4.78±0.10
H10A	H10B	-	5.80±0.10
C12	C4	0.28±0.10	0.28±0.10
C13	H13A	-1.23±0.10	-
C13	H13B	0.27±0.10	-
C14	C11	0.14±0.10	0.14±0.10
C15	C11	0.16±0.10	0.14±0.10

Table SI-2. NMR signals assignment and RDCs of $\beta\beta$ -conformer of BCP.

NMR attribution			
C	δ_C , ppm	H	δ_H , ppm
C1	55.7	H1	1.49
C2	31.3	H2A	1.67
		H2B	1.55
C3	34.7	H3A	1.57
		H3B	2.51
C4	135.1	-	-
C5	124.4	H5	5.26
C6	29.3	H6A	2.42
		H6B	2.11
C7	40.2	H7A	1.9
		H7B	2.42
C8	155.0	-	-
C9	49.3	H9	2.24
C10	42.5	H10A	1.78
		H10B	1.56
C11	32.6	-	-
C12	22.1	H12	1.58
C13	110.8	H13A	4.88
		H13B	4.95
C14	21.9	H14	0.96
C15	29.7	H15	0.97

Coupling nuclei		$^1D_{\text{exp}}$, Hz	
		CLIP HSQC	F_1 -cpd HSQC (MQ evol.)
C1	H1	4.03±0.20	3.83±0.10
C2	H2A	Str. Coupl.	no
C2	C2B	Str. Coupl.	no
C3	H3A	Str. Coupl.	3.24±0.20
C3	H3B	Str. Coupl.	no
C5	H5	2.54±0.20	2.99±0.20
C6	H6A	2.40±0.30	2.72±0.50
C6	H6B	0.70±0.30	0.62±0.50
H6A	H6B	-	3.22±0.05
C7	H7A	overlap	3.61±0.20
C7	H7B	-0.54±0.20	no
C9	H9	3.88±0.30	3.84±0.30
C10	H10A	1.00±0.20	1.17±0.10
C10	H10B	2.75±0.15	2.68±0.10
H10A	H10B	-	3.02±0.15
C12	C4	0.28±0.10	0.27±0.10
C13	H13A	-1.01±0.10	no
C13	H13B	-0.03±0.10	no
C14	C11	0.23±0.10	0.21±0.10
C15	C11	0.12±0.10	0.11±0.10

Cartesian coordinates for β -Caryophyllene conformers

Structural models for the RDC fits were generated computationally by geometry optimization using density functional theory as implemented in ORCA v3.0.1.^[9] While the previously published studies by Alagona et al.^[8] give some torsion angles, electronic energies and predicted NMR chemical shifts, no Cartesian coordinates of the conformers are reported.

Starting from a geometry used by Krupp et al.,^[10] bonds were rotated manually into geometries resembling the $\alpha\alpha$, $\beta\alpha$, $\beta\beta$ and $\alpha\beta$ conformers reported by Alagona et al. These starting geometries were subsequently re-optimized at the B3LYP/def2-TZVP^[11] level of theory. Numerical frequency analysis was performed to confirm the local minimum nature of the respective geometries. Table SI-3 compares the relevant torsion angles and relative conformer populations (derived from Boltzmann weighting) to those reported previously by Alagona et al. The $\alpha\beta$ geometry is not expected to be populated significantly at room temperature and is not observed in the NMR measurements.

Table SI-3. Comparison of DFT-optimized geometries calculated in this work with those reported previously by Alagona et al. (values given in parentheses).

Conformer	C6-C7-C8-C13 torsion (deg.)	C2-C3-C4-C12 torsion (deg.)	ΔE (kJ/mol) ^a	Boltzmann population (%)
$\alpha\alpha$	87.8 (84.5)	81.9 (82.6)	0.000 (0.000)	47.53 (54.12)
$\beta\alpha$	-82.2 (-81.3)	83.2 (81.1)	0.847 (1.849)	33.77 (25.67)
$\beta\beta$	-97.0 (-91.5)	-128.6 (-126.0)	2.313 (2.443)	18.69 (20.20)
$\alpha\beta$	83.4 (86.4)	-102.2 (-129.5)	21.543 (20.815)	0.01 (0.01)

^a relative electronic energies. Values given by Alagona et al. in kcal/mol were converted to kJ/mol for comparison.

$\alpha\alpha$ conformer

C7	-1.73327117181850	-1.77820500473941	-2.29115863301432
C8	-0.55731003654020	-1.25536028276519	-3.09905280774412
C9	-0.33043548619936	0.22638049769772	-3.30908913452871
C5	-1.01520493064994	-0.80056308555655	-0.13342594362439
C6	-1.37350907977576	-2.08575508360322	-0.80721666770035
C1	-0.67300379386680	1.38202548689861	-2.31061657877904
C2	0.35954063456868	1.89821529884217	-1.30488548860629
C3	0.26902823697989	1.25469593142328	0.10668030010963
C4	0.19363029755245	-0.24480974221335	-0.01581853892338
C12	1.50575316548968	-0.95693333492627	-0.20498648187083
C13	0.25583537748238	-2.12315105915667	-3.70450967708168
C10	-1.23073606637242	0.94667597089612	-4.35097506771688
C11	-1.09043124340522	2.26568592374780	-3.54042416913712
H1	-1.59521167634404	1.13598449124328	-1.78046249932595
H9	0.70941687518397	0.35251616517380	-3.62207492603027
C14	0.02966508707956	3.14665721977439	-4.09697789398944
C15	-2.36260151002627	3.08135505366122	-3.33952811931179
H7A	-2.55795173561613	-1.05936843578192	-2.31059531678714
H7B	-2.10735207605629	-2.69400409990509	-2.75579636040319
H5	-1.86892467924200	-0.15539373366167	0.06406458596873
H6B	-0.55759128390755	-2.80900656303050	-0.78221641834107
H6A	-2.23811210252789	-2.55697046102717	-0.33034175491040
H2B	1.36633828609280	1.75463559386485	-1.70837167352474
H2A	0.22989767014925	2.97914911206761	-1.18791667596750
H3B	1.12796257618416	1.57950033778565	0.70219580068061
H3A	-0.62825070344715	1.63065156747542	0.60433027616655
H12A	2.08808382509718	-0.50934784490737	-1.01553498350857
H12B	2.11151887688243	-0.85850243727142	0.70224747443019
H12C	1.39164347639609	-2.01669374630205	-0.42445605154082
H13A	0.08114065745805	-3.19260949411664	-3.66402600804785

H13B	1.11774474526898	-1.79401872273056	-4.27333806834121
H10A	-2.25513101045426	0.56777524018126	-4.33220958094461
H10B	-0.86952419085276	0.94066607902244	-5.38140123703370
H14A	-0.27458886661807	3.58059345468003	-5.05354493989939
H14B	0.26390866421556	3.97312758208381	-3.42148088309094
H14C	0.95043759479750	2.58602479355081	-4.26875235972526
H15A	-2.70080374753930	3.53067735501958	-4.27830869885406
H15B	-2.19881880165773	3.89725364365110	-2.62849350760117
H15C	-3.17269185396099	2.45879633295410	-2.95190129144954

$\beta\alpha$ conformer

C7	-1.52461282047094	-2.02975048080262	-2.16023003190019
C8	-2.13318237918140	-0.76049396847212	-2.74896824185690
C9	-1.19620787061045	0.31222653833295	-3.27876837923890
C5	-1.04267179737108	-0.66286037097979	-0.14754147954163
C6	-1.45323439049373	-2.02955163605179	-0.60615448085287
C1	-0.86554700359287	1.64677922606555	-2.49121454022774
C2	0.40765351544324	1.83199575167136	-1.65644345055236
C3	0.34011463896438	1.34858906286205	-0.18841816331683
C4	0.18762764064999	-0.14985645088892	-0.13178118159954
C12	1.45327695560262	-0.95542928448273	-0.24777246136025
C13	-3.45986800656598	-0.64110633212671	-2.80329101454161
C10	-1.68102243082437	1.19526711789494	-4.45731095854899
C11	-0.96035249487477	2.43045333371714	-3.85317252371436
H1	-1.73802592254568	1.91135245872689	-1.88646468849265
H9	-0.25011902765376	-0.16450163918916	-3.54894035943800
C14	0.38616046971237	2.68815541496283	-4.53128272642951
C15	-1.77383238372947	3.71867945341134	-3.80238752449361
H7A	-2.09995606986641	-2.89689424770825	-2.49400709267814
H7B	-0.51205840452958	-2.15346514320492	-2.55254429548653
H5	-1.86607235855148	0.03770611501441	-0.04158790094153
H6B	-0.76477337034172	-2.81119767983090	-0.27884010347585
H6A	-2.43664711278228	-2.28120850912685	-0.20241625399864
H2B	1.24842547252312	1.34339031907476	-2.15755430673450
H2A	0.65126112446403	2.90082722056912	-1.64503143196804
H3B	1.24482742055762	1.67916086520926	0.33216384351575
H3A	-0.50818152114691	1.83133351803821	0.30443155460915
H12A	2.13503237546505	-0.69891902106624	0.56934458643617
H12B	1.27239731627166	-2.02900105526426	-0.20572008176145
H12C	1.99109865244997	-0.73829262578594	-1.17680977466344
H13A	-4.10882978000505	-1.42920445433687	-2.43861450090388
H13B	-3.95491509242687	0.23387053658423	-3.20465019616956
H10A	-2.76239647607136	1.32416748774788	-4.45555059670058
H10B	-1.37430119530111	0.87596296891344	-5.45570827120504
H14A	0.22667421018271	3.06698296738460	-5.54486790833736
H14B	0.97509939633999	3.43433933045855	-3.99287819083719
H14C	0.98965487028835	1.78141522974029	-4.60961411462913
H15A	-1.94128903309584	4.11846995124086	-4.80726977750257
H15B	-1.25582184718618	4.49058988234112	-3.22457156296798
H15C	-2.74872826969581	3.55191714935629	-3.33879041749375

$\beta\beta$ conformer

C7	-1.90773413165683	-1.87863935969646	0.78482927799605
C8	-0.72072985527074	-1.72456936394926	-0.15558075242551
C9	0.50843678015151	-0.99197122392147	0.35667366220537
C5	-2.13187024169230	0.59472749447167	0.88988910394223
C6	-2.90071213546240	-0.68060307705116	0.78389718142791
C1	0.96113647845628	0.43532475545869	-0.15323129729299
C2	0.58429758488965	1.74056711200507	0.55833862497638
C3	-0.70638028792629	2.42750423425233	0.06879988198031
C4	-1.87113839270055	1.46643987908686	-0.08362023890867
C12	-2.56898089628030	1.50563034396381	-1.41536119564006
C13	-0.76301192205143	-2.28519513413909	-1.36417995751579
C10	1.91706976935923	-1.50665212903988	-0.04520177050518
C11	2.45098445028248	-0.05144280900715	-0.05280141924948
H1	0.70529526371138	0.51223497893496	-1.21466287317156
H9	0.44990553514081	-0.95606111562481	1.44710261543425
C14	3.13048119266748	0.29062730188434	1.27626863829126

C15	3.34100478557813	0.33351605120461	-1.22694625002745
H7A	-2.46245579279334	-2.78457326739115	0.52912702903793
H7B	-1.53019510033867	-2.01997479168227	1.80286828935637
H5	-1.55925729067181	0.69265201138371	1.80966684568204
H6B	-3.59727906820112	-0.81099332268111	1.61908624961394
H6A	-3.49010565570971	-0.71183184393555	-0.13248354423082
H2B	1.40590928290888	2.45147012958680	0.41549293214340
H2A	0.52672463254375	1.56762499304100	1.63636011347620
H3B	-0.95548560825055	3.25326634279058	0.74452045079236
H3A	-0.50970913687477	2.89031056030069	-0.90269392984789
H12A	-3.43511599681659	0.84869678803454	-1.47204263636483
H12B	-2.90926405453817	2.52458252905280	-1.62896482866948
H12C	-1.88119023157453	1.23008678641987	-2.22175958241814
H13A	-1.63862845717598	-2.82730753499917	-1.70189851974508
H13B	0.05981168607568	-2.22794581683710	-2.06610376313724
H10A	2.39414412398298	-2.20969733493845	0.64065949905242
H10B	1.92491429062115	-1.94029603564136	-1.04528851706797
H14A	4.08024827122351	-0.24546883440872	1.35478814087805
H14B	3.34653157866459	1.35830303796281	1.36454217284937
H14C	2.51896956771226	0.00249366355966	2.13360825620348
H15A	4.30815121734041	-0.17581405874186	-1.17478340242539
H15B	2.87296742769319	0.06493286226088	-2.17707626545085
H15C	3.53578033698274	1.41080519803033	-1.24283822124495

$\alpha\beta$ conformer

C7	-1.24165530043525	-1.59164319382940	0.53450049421032
C8	-0.14915184898231	-1.06718303334593	1.45179369672242
C9	1.03262051516936	-0.29661589522521	0.89889075283087
C5	-2.02589931643742	0.75771114154802	0.34416992479383
C6	-2.49105787322033	-0.65901878956609	0.49440561046641
C1	1.03792409380851	0.59375199857654	-0.39053433318498
C2	0.73399186080484	2.09980001196412	-0.33256248123430
C3	-0.72959279655122	2.55424200563605	-0.68965117003640
C4	-1.69448035272996	1.39097787605995	-0.78110821529000
C12	-2.05936970317876	0.93136615543871	-2.16612858299628
C13	-0.20864671352927	-1.31300540464589	2.76175646950877
C10	2.19592091700360	-1.10692942619292	0.25786579351957
C11	2.50483350932434	0.10044862011113	-0.67136723526628
H1	0.41101261979259	0.11498945414384	-1.14394937823132
H9	1.44490011292576	0.29519737752746	1.71956579141966
C14	3.60105229361598	0.99501161843945	-0.08783407976320
C15	2.82291489284897	-0.21817938193433	-2.12826500724938
H7A	-0.85789106831644	-1.69938631935445	-0.48288567943931
H7B	-1.55380379920688	-2.58557932091306	0.86475581887322
H5	-1.69524706481880	1.21429527748751	1.27391109300848
H6B	-3.04709394214060	-0.77841254912609	1.42755246641039
H6A	-3.14979931101773	-0.97914974884052	-0.31525871694922
H2B	1.42185409227415	2.61479341970808	-1.00877423610614
H2A	0.98272904191568	2.46649891806594	0.66653244098422
H3B	-1.07033057055589	3.26227995724156	0.06897513972720
H3A	-0.71406400655018	3.10357239350916	-1.63351518125744
H12A	-2.74964712355643	0.08846286689154	-2.16908930437680
H12B	-1.17246962666431	0.64641072915038	-2.74268778908571
H12C	-2.53139057192081	1.75133164851877	-2.71717866375213
H13E	-0.99612149837217	-1.92047744809933	3.19373363023650
H13Z	0.53219610376439	-0.91961993959164	3.44885816913507
H10A	2.98398450452856	-1.44909196481883	0.93182361156144
H10B	1.82189423239930	-1.96372215465022	-0.30680761907381
H14A	4.56129104109809	0.47248083944671	-0.12429959621022
H14B	3.70889160082628	1.91909437860474	-0.66071660357918
H14C	3.41063034796424	1.27066835172966	0.95153864071054
H15A	3.78066387040693	-0.73991816741564	-2.21952127339765
H15B	2.05532846729386	-0.85549241867308	-2.57352593377348
H15C	2.89216837041926	0.69558011642327	-2.72679846386566

RDC cross-fits:

$\beta\beta$ -BCP RDCs fitted to Cartesian coordinates of either $\alpha\alpha$ conformer or $\beta\alpha$ conformer

The results show that the RDC data of the $\beta\beta$ conformer are described the best with the Cartesian coordinates of $\beta\beta$ conformer (as judged from the lowest quality factor, see the main manuscript text). The cross fitting to the coordinates of other conformers give worse quality factors Q .

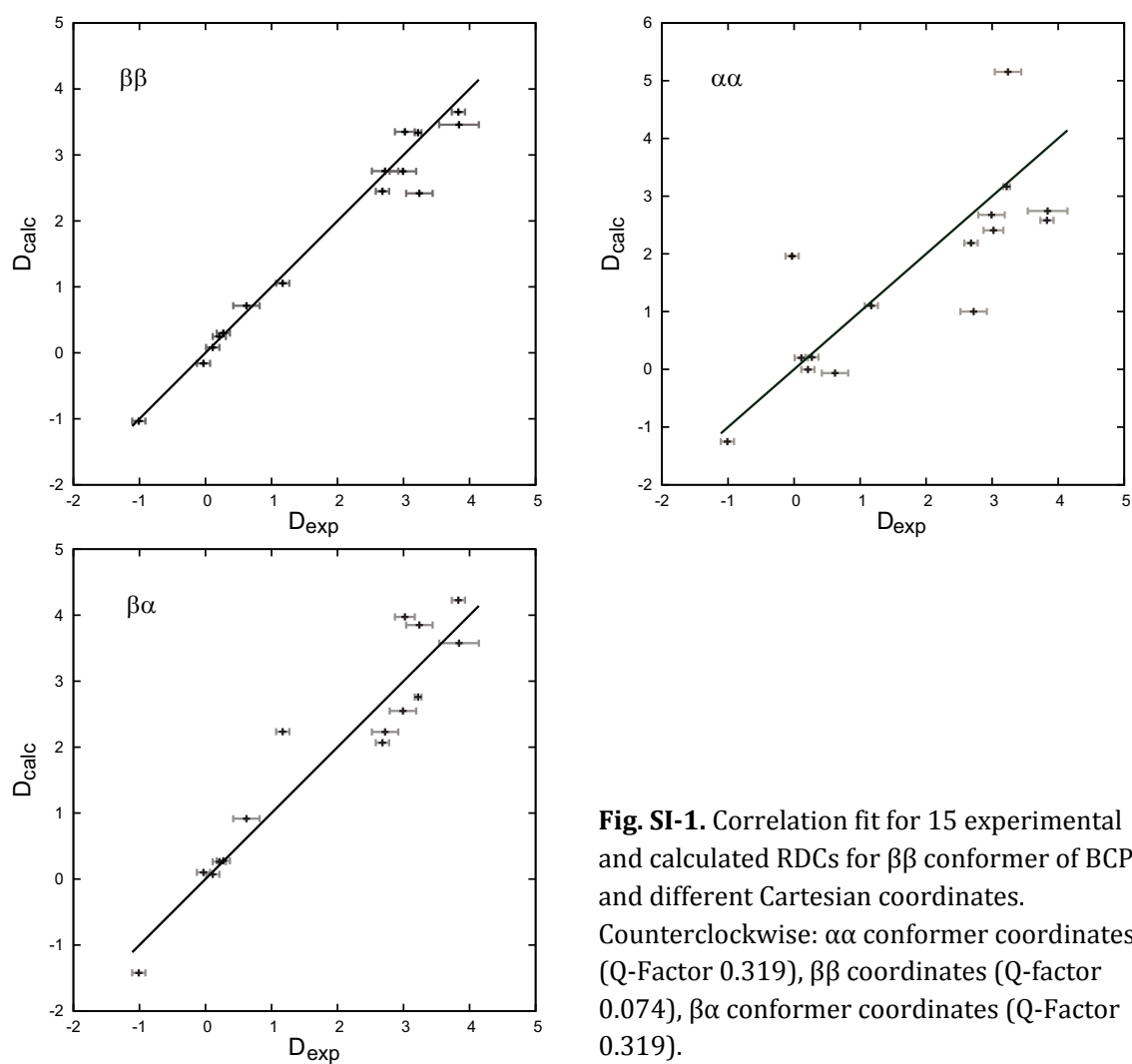


Fig. SI-1. Correlation fit for 15 experimental and calculated RDCs for $\beta\beta$ conformer of BCP and different Cartesian coordinates. Counterclockwise: $\alpha\alpha$ conformer coordinates (Q-Factor 0.319), $\beta\beta$ coordinates (Q-factor 0.074), $\beta\alpha$ conformer coordinates (Q-Factor 0.319).

Anisotropic alignment study of (+)-isopinocampheol and its acetyl ester

Isopinocampheol (IPC) has been traditionally used as a test small molecule for the performance of new alignment media in our and other groups developing RDC methods for small organic molecules. Technically, one can prepare an aligned sample in two ways. First, the gel can be pre-swollen in pure solvent up to its equilibration point, when neither length nor $\Delta\nu_Q$ of the gel changes anymore. The solution of a small molecule is then applied on the top of a pre-swollen gel and allowed to diffuse. The second option is to achieve simultaneous gel equilibration and analyte diffusion. The latter approach implies that the degree of alignment of a gel in the pure solvent is known.

We prepared samples either by simultaneous gel swelling and diffusion of the small molecule or diffusion of (+)-IPC into pre-swollen PDMS gel being applied in solution on the top of the gel. In both cases degradation of $\Delta\nu_Q$ was observed, seen in ^2H NMR spectra and images (Fig. SI-2).^[12] For the sample, in which (+)-IPC diffused from the top of the gel, ^2H NMR images indicate a $\Delta\nu_Q$ reduction at the analyte location, propagating together with (+)-IPC diffusion (Fig. SI-3).

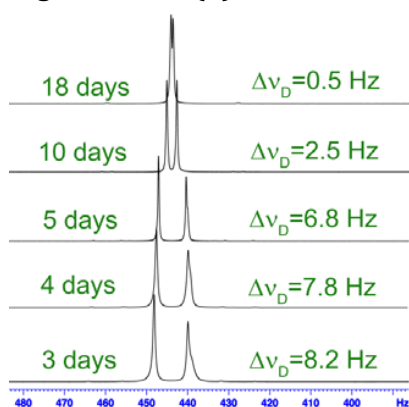


Fig. SI-2. ^2H NMR spectra (400 MHz): simultaneous swelling-diffusion of a 1.3 mol% PDMS gel in 8 mg (+)-IPC/1 mL CDCl_3 solution. The analyte diffusion in course of gel swelling is characterized by $\Delta\nu_Q$ reduction (the value of $\Delta\nu_Q$ in pure solvent is ca. 23 Hz).

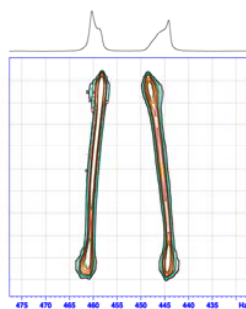


Fig. SI-3. ^2H NMR image (400 MHz) of a gel when (+)-IPC/ CDCl_3 was added on the top of a pre-swollen gel. We observed $\Delta\nu_Q$ degradation for 1 and 1.3 mol% PDMS gels, commencing with the analyte diffusion (top of the graph corresponds to the top of the NMR tube).

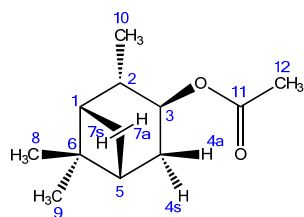
We observed an elongation of the gel in (+)-IPC solution to the values higher than those seen in pure CDCl₃. This process was accompanied by gradual reduce of $\Delta\nu_Q$ until the value of 0 Hz was reached, which is characteristic for isotropic systems. Moreover, a PDMS gel contacted with (+)-IPC for more than one month shortened in length and released viscous liquid, which later on became significantly fluid. The gel could either shrunk or depolymerize in the (+)-IPC solution at the concentrations of 9 mg/mL. The ²⁹Si 1D and 2D NMR examination of the liquid, released from an (+)IPC/PDMS/CDCl₃ sample, evidences for the polymer chemical degradation: both liquid and an intact gel show a ²⁹Si NMR signal of dimethylsiloxanes at -21 ppm (**Fig. SI-6**) A 7-month old sample became completely isotropic.

Interaction of PDMS with IPC

The chemical degradation of PDMS gel in the fine solutions of (+)-IPC was surprising for us, especially because similar sticks earlier were reported to be successfully applied in a number of studies^[13] but not for isopinocampheol. A synthesized (+)-IPC-derivative, O-capped with acetyl group, did not prevent the reduction of the $\Delta\nu_Q$ but degradation seemed to slow down such that we were able to get 10 RDCs (in the range -4...+2 Hz) already after two days of diffusion. The experimental and theoretical RDC values are in agreement with the spatial structure of the molecule (**Table SI-4** and **Fig. SI-4**).

The ability of PDMS to swell differently in solvents is of great concern in the development of micro devices and their components. Alcohols are not reported to be good solvents for PDMS, i.e. do not show high values of volume increase^[14]. Thus, our results showing the independence of PDMS gel extension from alcohol or ester functionalities of (+)-IPC, on the one hand, coincide well with the general data for the polymer swelling properties. On the other hand, the information on chemical incompatibility of (+)-IPC and PDMS is potentially of big importance for further applications.

(+)-Isopinocampheol acetate ((+)-IPC-OAc). 1M solution of (+)-isopinocampheol in



pyridine was chilled on an ice bath and 2 eq. of acetic anhydride were added via septum. The reaction mixture was stirred for 5 hrs. on the ice-bath and then kept in a fridge until reaction completion. The reaction progress was monitored via TLC. The mixture then was poured on an ice cold HCl solution and the product was extracted in diethyl ether. The combined organic

extractions were washed with 1M HCl, water and brine. The final ether solution was dried over MgSO₄ and the organic solvent was removed on a rotary evaporator providing dark-yellow liquid. Yield: 80%. R_f (EtOAc-PE, 1:5) 0.6. ¹H NMR (400 MHz, CDCl₃, 300 K) δ = 0.89 (CH₃-9, 3H, s), 0.98 (H-7a, 1H, d, 9.9 Hz), 1.02 (CH₃-10, 3H, 7.4 Hz), 1.15 (CH₃-8, 3H, s), 1.58 (H-4a, 1H, ddd, 14.3x4.2x2.8 Hz), 1.75 (H-1, 1H, dd, 5.9x2.1 Hz), 1.86 (H-5, 1H, m), 1.99 (Ac-12, 3H, s), 2.04 (H-2, 1H, m), 2.30 (H-7s, 1H, m), 2.52 (H-4s, 1H, m), 4.96 (H-3, 1H, m) ppm. ¹³C NMR (100 MHz, CDCl₃, 300 K) δ = 20.5 (CH₃-10), 21.5 (Ac-12), 23.7 (CH₃-9), 27.5 (CH₃-8), 33.4 (C-7), 35.9 (C-4), 38.3 (C-6), 41.3 (C-5), 43.6 (C-2), 47.5 (C-1), 74.1 (C-3), 177.0 (CO-11) ppm.

RDC structure elucidation for (+)-IPC-OAc

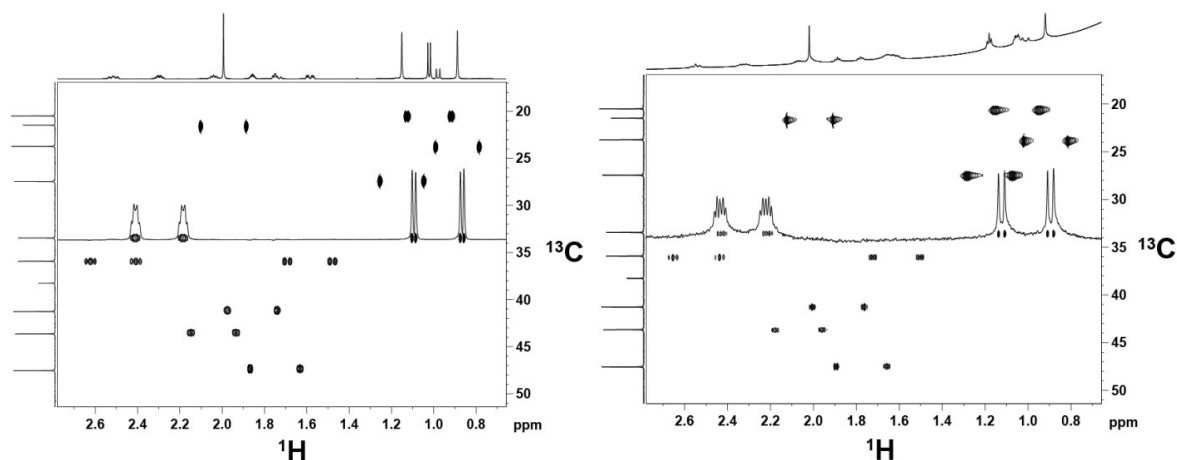


Fig. SI-4. Fragments of a CLIP HSQC spectrum (600 MHz) of (+)-IPC-OAc in CDCl_3 (left) and a spectrum of (+)-IPC-OAc recorded in 2.6% PDMS equilibrated in CDCl_3 (right). Selected 1D-slices of the F1-domain corresponding to diastereotopic protons **H7s** and **H7a** reveal high quality of the acquired data for the anisotropic spectrum.

Table SI-4. RDC data for IPC-OAc

H atom	C atom	$^1D_{\text{exp}}$ Hz (CLIP HSQC)
1	1	0.05 ± 1.00
2	2	1.41 ± 0.20
3	3	-0.21 ± 0.30
4s	4	0.65 ± 0.20
4a	4	1.73 ± 0.30
5	5	2.32 ± 0.70
7s	7	-3.98 ± 0.50
7a	7	-0.02 ± 0.20
8*	6	-0.32 ± 0.10
9*	6	0.05 ± 0.05
10*	2	0.20 ± 0.40

* C atom

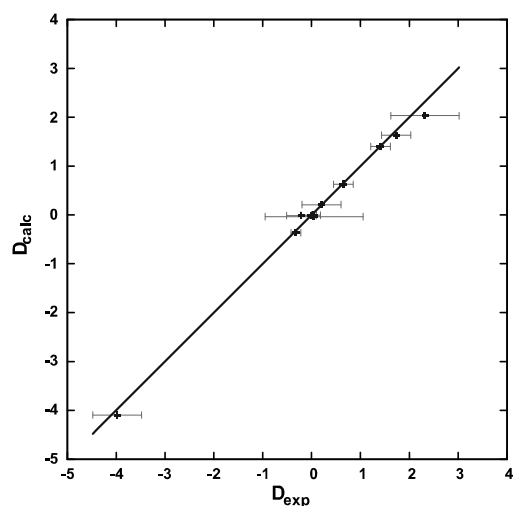


Fig. SI-5. Correlation between calculated and experimental RDCs for (+)-IPC-OAc (Q-factor 0.108).

NMR Studies of PDMS-decomposition



In our experiments on PDMS gels equilibration with (+)-IPC and its acetyl ester we noticed the reduction of the length and decrease of the $\Delta\nu_Q$ of the alignment medium. The same behavior is true not only for our chemically synthesized PDMS gels but also for a sample prepared by β -irradiation^[10a]. On the photo (**Figure SI-6**) one can see the first step of visible gel changes, when it starts to be fluid. To probe whether chemical degradation or gel shrinkage took place, we analysed by NMR spectroscopy methods the ‘supernatant’ – the liquid above the gel level.

Figure SI-6. Photography of dissolving PDMS gel in IPC/ CDCl_3 solution

^{29}Si NMR spectroscopy of PDMS and oligodimethylsiloxanes

The ‘supernatant’ solution in CDCl_3 was analysed by 1D and 2D ^{29}Si NMR spectroscopy. In (^1H - ^{29}Si) HMBC spectra of the liquid released from the (+)IPC/PDMS/ CDCl_3 anisotropic system (**Fig. SI-7a**) and spectra of the intact PDMS/ CDCl_3 (**Fig. SI-7b**) one can clearly see that ‘supernatant’ contains dimethylsiloxanes (-22 ppm in ^{29}Si), i.e. chemical changes occur leading to the loss of the anisotropic properties of the gel. Measurements were performed on Avance-III-600 NMR spectrometer.

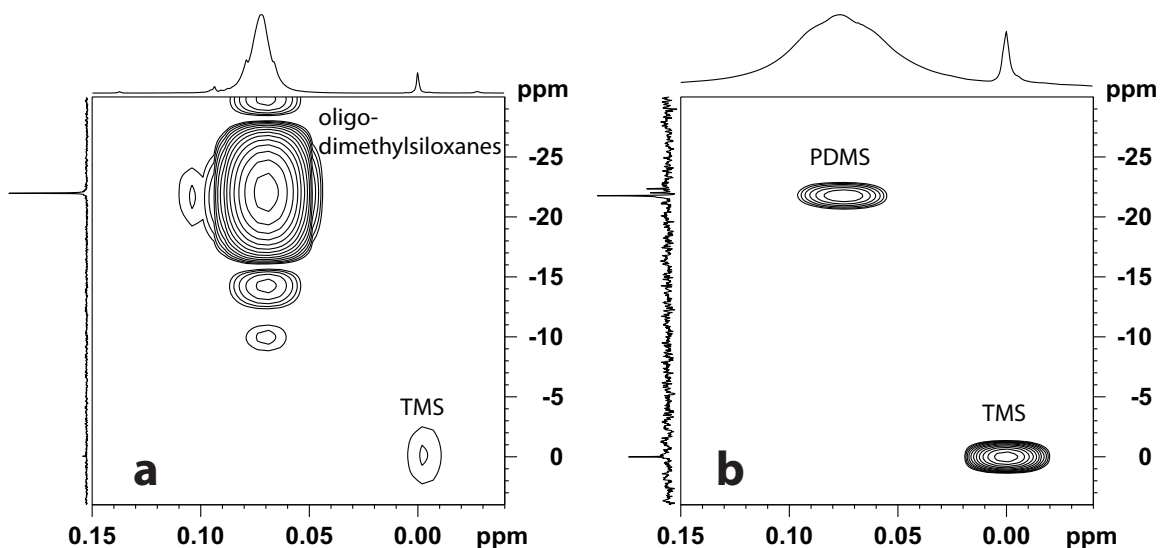


Fig. SI-7. (^1H - ^{29}Si) HMBC spectra of the depolymerized PDMS (a) and an intact gel (b).

DOSY-study of PDMS-decomposition.

A 2D DOSY spectrum (Bruker pulse program *stebpgp1s*, $\Delta = 200\text{ms}$, $\delta = 2\text{ ms}$, linear gradient 2-95% in 32 incremental steps, G_{max} of the probe head in the z-direction is 50 G cm^{-1})^[2] of the 'supernatant' solution of a (1% PDMS gel/(+)-IPC) was obtained at 300 K on Avance-III HD-400 spectrometer (see **Figure SI-8**). The self-diffusion coefficients D of TMS, (+)-IPC, residual CHCl_3 and oligodimethylsiloxanes were determined via standard monoexponential fitting analysis in Topspin 3.2. With $D = 1.93 \cdot 10^{-9}\text{ m}^2\text{s}^{-1}$, the experimental value for TMS in CDCl_3 is lower as compared to the measured at the same temperature previously published^[15] value of $2.92 \cdot 10^{-9}\text{ m}^2\text{s}^{-1}$, which might be due to the presence of high content of oligomers in the mixture and thus a higher viscosity. For the depolymerized PDMS gel the estimated range of D is about $(2.00\text{-}2.76) \cdot 10^{-11}\text{ m}^2\text{s}^{-1}$, i.e. two orders lower values than TMS corresponding to much slower diffusion. Unfortunately, the more precise determination of the self-diffusion coefficient, which could allow a determination of the molecular weight of the depolymerisation products, was not possible due to the broad MW distribution of the oligodimethylsiloxanes.

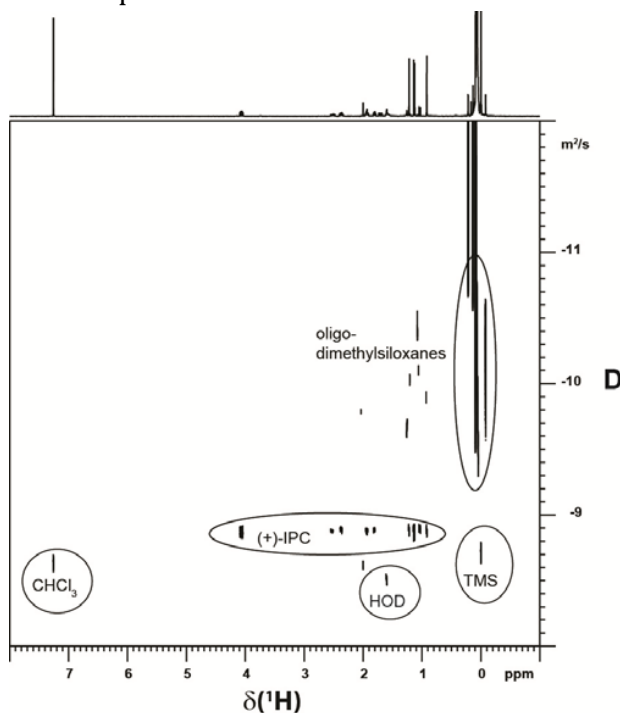


Fig. SI-8. ^1H DOSY experiments confirm the presence of the de-polymerization products in CDCl_3 solution.

Thus chemical incompatibility of the PDMS gels and the bicyclic monoterpene (+)-isopinocampheol lead to chemical degradation of the gel, as seen in ^2H NMR, ^{29}Si NMR spectra and ^1H DOSY experiments. Esterification of the alcohol functionality allows performing RDC analysis but does not fully prevent degradation of anisotropic properties. The latter cannot be accounted for only by the alcohol functionality of the analyte. The reason for the chemical incompatibility of the polymer gel and the (+)-IPC ester is not yet known.

Predicting solvent quadrupolar splitting in a swollen gel

We consider a polymer network swollen by a deuterated solvent. Each molecule of solvent diffuses throughout the gel, interacting occasionally with the monomers of the polymer chains. During these encounters, the interactions between the partially aligned monomers of the chains and the solvent bias the orientation of the solvent molecule. The quadrupolar splitting of the solvent can thus be written as:

$$\Delta\nu_Q = \Delta\nu_Q^0 \varepsilon \phi S \quad (1)$$

where ϕ is the chain monomer volume fraction accounting for the probability of a solvent molecule to encounter a chain monomer, S is the average of the second Legendre polynomial of monomer orientations, $\Delta\nu_Q^0$ is the quadrupolar splitting of perfectly aligned solvent molecules (for instance $\Delta\nu_Q^0=168$ kHz ^[16] for CDCl_3) and ε is an efficiency factor accounting for the transfer of orientation between the monomers and the solvent molecules during a solvent-monomer encounter. Equation (1) can be equivalently understood by considering the time average of the second Legendre polynomial of solvent orientations. When the molecule diffuses freely away from the polymer chains, the molecular orientation state is described by an isotropic orientation distribution, and the measure of the second Legendre polynomial is averaged to zero. During a fraction ϕ of the total average time, when the solvent encounters a monomer of the polymer chain, its distribution is biased proportionally to the orientation state of the chain monomers. The efficiency of solvent orientation during this time fraction is a function of the detailed microscopic interactions between the chain monomers and the solvent molecules. Maximal quadrupolar splitting of the solvent $\Delta\nu_Q = \Delta\nu_Q^0$ would require thus small amounts of solvent $\phi \cong 1$, completely aligned chains $S = 1$ and a perfectly efficient transfer of orientations $\varepsilon = 1$. Note that while ϕ and S are determined by the experimental conditions, ε is an intrinsic property of a given solvent/monomer pair. Tabulated values of ε for different solvent/monomer pairs would therefore allow predicting the expected quadrupolar splitting for experiments performed under controlled swelling and stretching conditions. In the following we first review theoretical predictions for S in stretched polymer gel networks, then provide explicit expectations in the case where gel stretching is caused by swelling in a tube. Finally, we compare our predictions with the data from the experiments discussed in this paper and extract the value of the orientation transfer efficiency for the pair PDMS/ CDCl_3 .

Orientation of chain monomers in a polymer gel. We first write (following Sommer & Saalwächter ^[17]) the order parameter of the chain monomers as

$$S = \frac{R^2}{R_0^4} \quad (2)$$

Where R is the end-to-end distance of a polymer chain of N monomers connecting two cross-linking points and R_0 the average size of that chain in a given reference polymer solution with the same monomer volume fraction. Note that the average value of N is

related to the crosslinking molar fraction X_{CR} by $N = 2/(z X_{CR})$ where z is the crosslinker functionality. In our case where $z = 4$ one has $N = 1/(2 X_{CR})$.

We have, respectively for the ideal chain and for Flory excluded volume conditions

$$S_{id} = \frac{1}{N} \phi^{-2/3} \quad \text{and} \quad S_F = \frac{1}{N} \phi^{-1/6} \quad (3)$$

When the gel swells isotropically in an excess of solvent the prediction for the equilibrium volume fraction is

$$\phi_{id}^{eq} = N^{-3/8} \quad \text{and} \quad \phi_F^{eq} = N^{-3/5} \quad (4)$$

so that

$$S_{id}^{eq} = (\phi_{id}^{eq})^2 \quad \text{and} \quad S_F^{eq} = (\phi_{id}^{eq})^{3/2} \quad (5)$$

A molecule of solvent diffusing in a polymer gel probes many chain orientations during the NMR typical times (10^{-6} s), resulting in a vanishing average for the order parameter S . However, if one stretches the gel, a stress-induced anisotropy results that, for the case of uniaxial deformations along the Z-direction (R_x, R_y, R_z) \rightarrow ($R_x \lambda^{-1/2}, R_y \lambda^{-1/2}, R_z \lambda$), can be written as

$$S = \frac{R^2}{R^0{}^4} \left(\lambda^2 - \frac{1}{\lambda} \right) \quad (6)$$

with corresponding values for S resulting from different solvent conditions (ideal versus good solvent) following from (3) and (5).

Swelling in a tube. A typical NMR experiment is performed by inserting a cylindrical piece of a dry gel of diameter D_0 and length L_0 in an NMR tube of internal diameter D_T . The gel is then exposed to solvent and let swell to a length L . The polymer volume fraction ϕ is given by

$$\phi = \frac{D_0^2 L_0}{D_T^2 L} . \quad (7)$$

If the cylindrical dry gel had been allowed to swell isotropically in free solvent, it would swell to dimensions

$$D_I = D_0 \phi^{-1/3}$$

$$L_I = L_0 \phi^{-1/3}$$

By measuring the deformation λ with respect to the isotropically swollen state we get

$$\lambda = \frac{L}{L_I} = \frac{L}{L_0} \phi^{1/3} = \left(\frac{D_I}{D_T} \right)^2 = \left(\frac{D_0}{D_T} \right)^2 \phi^{-2/3} \quad (8)$$

Swelling of a gel in a tube then induces concomitantly a decrease of monomer volume fraction ϕ and an increase in anisotropy.

For a gel swollen in a tube we expect thus (from (1), (3), (6) and (8))

$$\Delta v_Q^{id} = \Delta v_Q^0 \varepsilon \frac{1}{N} \phi^{1/3} \left(\left(\frac{D_0}{D_T} \right)^4 \phi^{-4/3} - \left(\frac{D_T}{D_0} \right)^2 \phi^{2/3} \right) \quad (9a)$$

for ideal conditions and

$$\Delta v_Q^F = \Delta v_Q^0 \varepsilon \frac{1}{N} \phi^{5/6} \left(\left(\frac{D_0}{D_T} \right)^4 \phi^{-4/3} - \left(\frac{D_T}{D_0} \right)^2 \phi^{2/3} \right) \quad (9b)$$

for good solvent conditions. When the gel reaches maximum (equilibrium) swelling one gets

$$\Delta v_Q^{id,eq} = \Delta v_Q^0 \varepsilon \left(\left(\frac{D_0}{D_T} \right)^4 N^{-5/8} - \left(\frac{D_T}{D_0} \right)^2 N^{-11/8} \right) \quad (10a)$$

for ideal swelling and

$$\Delta v_Q^{F,eq} = \Delta v_Q^0 \varepsilon \left(\left(\frac{D_0}{D_T} \right)^4 N^{-7/10} - \left(\frac{D_T}{D_0} \right)^2 N^{-19/10} \right) \quad (10b)$$

for swelling under excluded volume. Note, that the maximum Δv achievable in a tube is given by

$$\Delta v_Q^{id,eq} = \Delta v_Q^0 \varepsilon \frac{6}{11} \left(\frac{5}{11} \right)^{5/6} \left(\frac{D_0}{D_T} \right)^9 \quad \text{for} \quad N = \left(\frac{11}{5} \right)^{4/3} \left(\frac{D_T}{D_0} \right)^8 \quad (11a)$$

and

$$\Delta v_Q^{F,eq} = \Delta v_Q^0 \varepsilon \left(\frac{D_0}{D_T} \right)^{15/2} \frac{12}{19} \left(\frac{7}{19} \right)^{7/2} \quad \text{for} \quad N = \left(\frac{19}{7} \right)^{5/6} \left(\frac{D_T}{D_0} \right)^5 \quad (11b)$$

Comparison with experiments. PDMS gels of diameter $D_0=3$ or 3.2 mm and length $L_0=14$ mm with different degrees of cross-linking (0.5, 1.0, 1.3, 1.5 and 2.0 mol% or, equivalently, $X_{CR} = 0.005, 0.010, 0.013, 0.015$ and 0.020 corresponding to $N=100, 50, 38, 33$ and 25) were swollen in NMR tubes with internal diameters $D_T=4.20$ mm for the two most cross-linked samples and $D_T=4.09$ for the three others. Swelling and equilibration of the gel is relatively fast, Δv_Q reaching stable values after one week for most cases. As the Fig. 1 in the main paper shows, all samples swollen for a period of four days or more exhibit homogeneous Δv_Q in the region captured by the NMR coil. The values of Δv_Q first increase with time, eventually reaching the plateau value of fully equilibrated gels.

We first plot in **Figs. SI-(9-12)** the bare data from PDMS sticks anisotropically swollen in an NMR tube, while one monitors the length of the gels and the values of quadrupolar splitting of CDCl_3 in ^2H NMR spectra. **Fig. SI-9** plots the increase in relative length L/L_0 of the gel sticks as a function of time. After a period of 20 to 40 days all samples have reached plateau conditions corresponding to maximum relative extensions in the range 2-4, with larger extensions being achieved for gels with smaller crosslinking fractions.

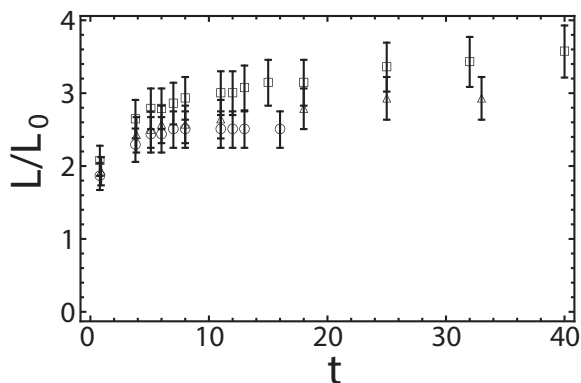


Fig. SI-9. Relative length L/L_0 as a function of time t , in days (0.5 mol% cross-linker - squares, 1.0 mol% - triangles, 1.3 mol% - circles).

For the relative extension values L/L_0 in **Fig. SI-9**, we display in **Fig. SI-10** the corresponding evolution of the monomer volume fraction in the gel, as given by Eq. (7). Under the experimental conditions of this paper, as the gels swell, they span monomer volume fractions from $\phi = 1$ in the dry state down to $\phi \cong 0.15$ for the less cross-linked samples in the fully swollen state.

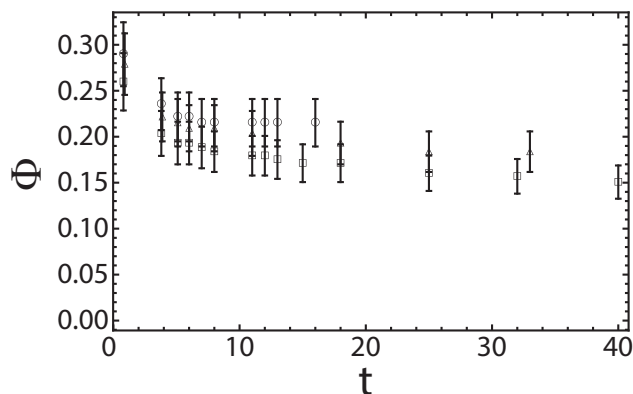


Fig. SI-10. Volume fraction ϕ of PDMS in a gel as a function of time t , in days (0.5 mol% cross-linker - squares, 1.0 mol% - triangles, 1.3 mol% - circles)

Fig. SI-11 shows the time evolution of the measured values for the quadrupolar splitting $\Delta\nu_Q$. Note that the measured quadrupolar splitting values are in the range 5-25 Hz, tens of thousand times smaller than the maximum possible values ($\Delta\nu_Q^0=168$ kHz) for perfectly aligned CDCl_3 molecules.

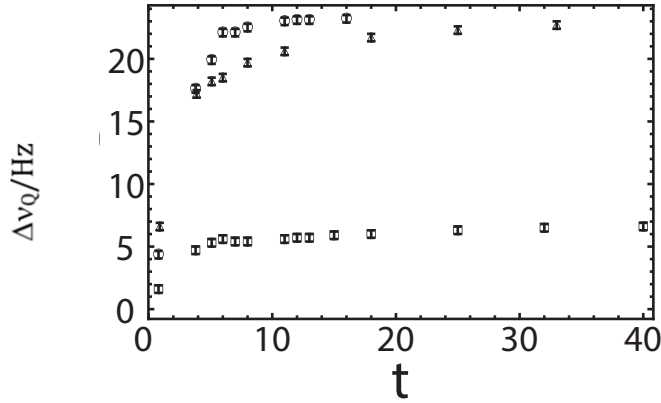


Fig. SI-11. Quadrupolar splitting Δv_Q in Hz as a function of time t , in days (0.5 mol% cross-linker - squares, 1.0 mol% - triangles, 1.3 mol% - circles)

We plot also in **Fig. SI-12** the evolution of quadrupolar splitting values Δv_D as a function of relative gel extension. The figure shows well that under these experimental conditions of constrained gel swelling, the measured Δv_Q values are not a function of chain stretching alone, since the larger stretching ratios, achieved for less cross-linked gels, do not translate into higher Δv_Q values.

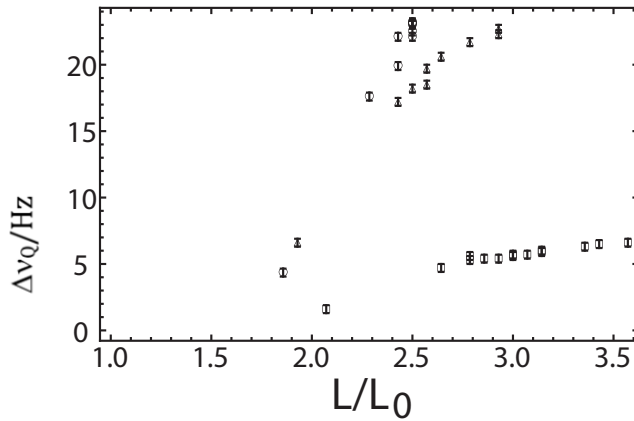


Fig. SI-12. Quadrupolar splitting Δv_Q in Hz as a function of relative length L/L_0 (0.5 mol% cross-linker - squares, 1.0 mol% - triangles, 1.3 mol% - circles)

We now analyze the bare data in **Figs. SI-(9-12)** according to the prescriptions of the theoretical arguments presented above. We first characterize the prevailing statistical conditions of the chains in the gel network, by plotting the equilibrium swelling fractions ϕ^{eq} in **Fig. SI-13** as a function of the molar cross-link fraction X_{CR} : we found that they follow the standard Flory-Rehner^[18] predictions for the swelling of gels in an ideal solvent - see Eq. (4) $\phi^{eq} \sim X_{CR}^{3/8}$. This shows that N , the average size of polymer strands between crosslinking points, spans a value range not large enough for reaching conditions where excluded-volume statistics applies. The larger value $N=100$ is obtained for the lower $X_{CR} = 0.005$, while the larger cross-linking fraction $X_{CR} = 0.02$ corresponds to $N=25$.

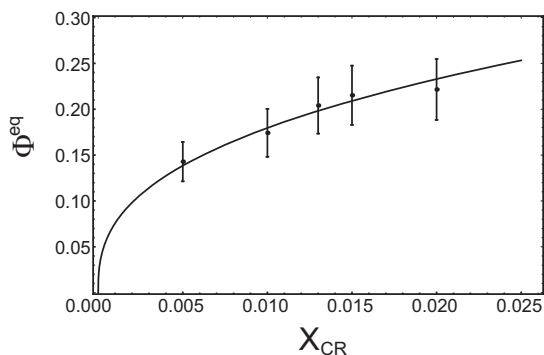


Fig. SI-13. Equilibrium volume fraction ϕ^{eq} of PDMS in a gel as a function of the molar fraction of the cross-linker X_{CR} . Note, that the average chain length N between two cross-linking points is given by $N = 1/(2 X_{CR})$ and thus varies here between $N=25$ for $X_{CR} = 0.02$ and $N=100$ for $X_{CR} = 0.005$. The line is the best power-law fit to the data $\phi^{eq} = 1.05 X_{CR}^{3/8}$.

We plot in **Fig. SI-14** Δv_Q as a function of polymer volume fraction for the five different X_{CR} values available. Interestingly, for samples with $N=50$ and $N=38$, ideal statistics provides the best fit with Eq. (9a), while for the largest N value, excluded volume statistics applies ^[19] as described in Eq. (9b). This is consistent with ideal swelling conditions applying throughout most of the explored cross-linking density range, the sample with $N=100$ being at the crossover between ideal and excluded volume statistics. For the two samples where only equilibrated properties have been measured $X_{CR} = 0.015$ and $X_{CR} = 0.020$, we assumed ideal conditions and extracted the corresponding ε values by assuming $\Delta v_Q^0 = 168$ kHz. Fitted ε efficiencies for the five samples range from $\varepsilon = 5.9 \times 10^{-3}$ to $\varepsilon = 7.1 \times 10^{-3}$.

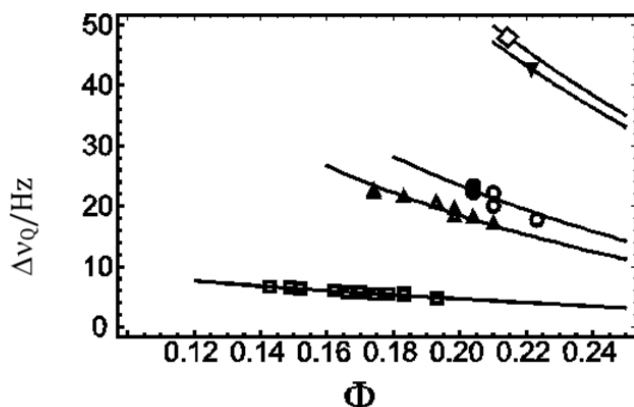


Fig. SI-14. Quadrupolar splitting Δv_Q in Hz as a function of the volume fraction ϕ . The lines are best fits according to the Eqs. (9) with $\Delta v_Q^0 = 168$ kHz, providing $\varepsilon = 6.5 \pm 0.5 \times 10^{-3}$ ((0.5 mol% cross-linker - squares, 1.0 mol% - triangles, 1.3 mol% - circles), 1.5 mol% - empty squares, 2.0 mol% - filled triangles)

Our results are thus well described by Eq. (1) and the associated ϕ dependent curves of Eqs. (9), confirming the physical picture developed above. In particular, it is clear from our data, that solvent quadrupolar splitting in gels swollen in a tube cannot be understood by gel stretching alone, since larger stretching is achieved for more diluted gels, where the probability of encounters between the solvent and the chain monomers is smaller. Our arguments account for the interplay between these two opposing effects and quantitatively describe the data. The analysis further stresses the importance of ε , the efficiency of transfer of the orientation from the monomers to the solvent molecules. This parameter, found here for PDMS and chloroform to be of the order of $1/150$, is expected for most systems to be an intrinsic property of a given solvent/monomer pair, but otherwise independent of experimental conditions. Anticipated exceptions are briefly discussed at the end of this section.

A clear picture emerges from our description that accounts for the quadrupolar splitting values observed under these experimental conditions. The reference value for solvent quadrupolar splitting, its maximum attainable value, is of order of a couple of hundred kilohertz. Dilution of the gel to the range of 10% volume fraction reduces this amount to the order of a couple of tens of kilohertz. Monomer orientation order parameters S , even for gels stretched in the tube by a factor four, do not rise about 0.2, bringing for these experimental conditions the maximum orientation power of the gel network to the range of a few thousand hertz. How much this orientation potential can be transferred to the solvent depends on the microscopic nature of the interactions between the monomers and the solvent during the time length of an encounter. We found here that such transfer is smaller than a percent for the PDMS/ CDCl_3 pair, bringing thus the final observed values to the range of a few tens of hertz.

In practice we expect, as values of the efficiency of orientation transfer will become available for other monomer/solvent pairs, that our approach will provide a widely applicable, quantitative pathway to understand and predict the amount of quadrupolar splitting that one can expect for a given experimental geometry. Indeed, given the efficiency of the gel/solvent pair, the simple knowledge of the gel size and cross-linking ratio will allow predicting quadrupolar splitting values.

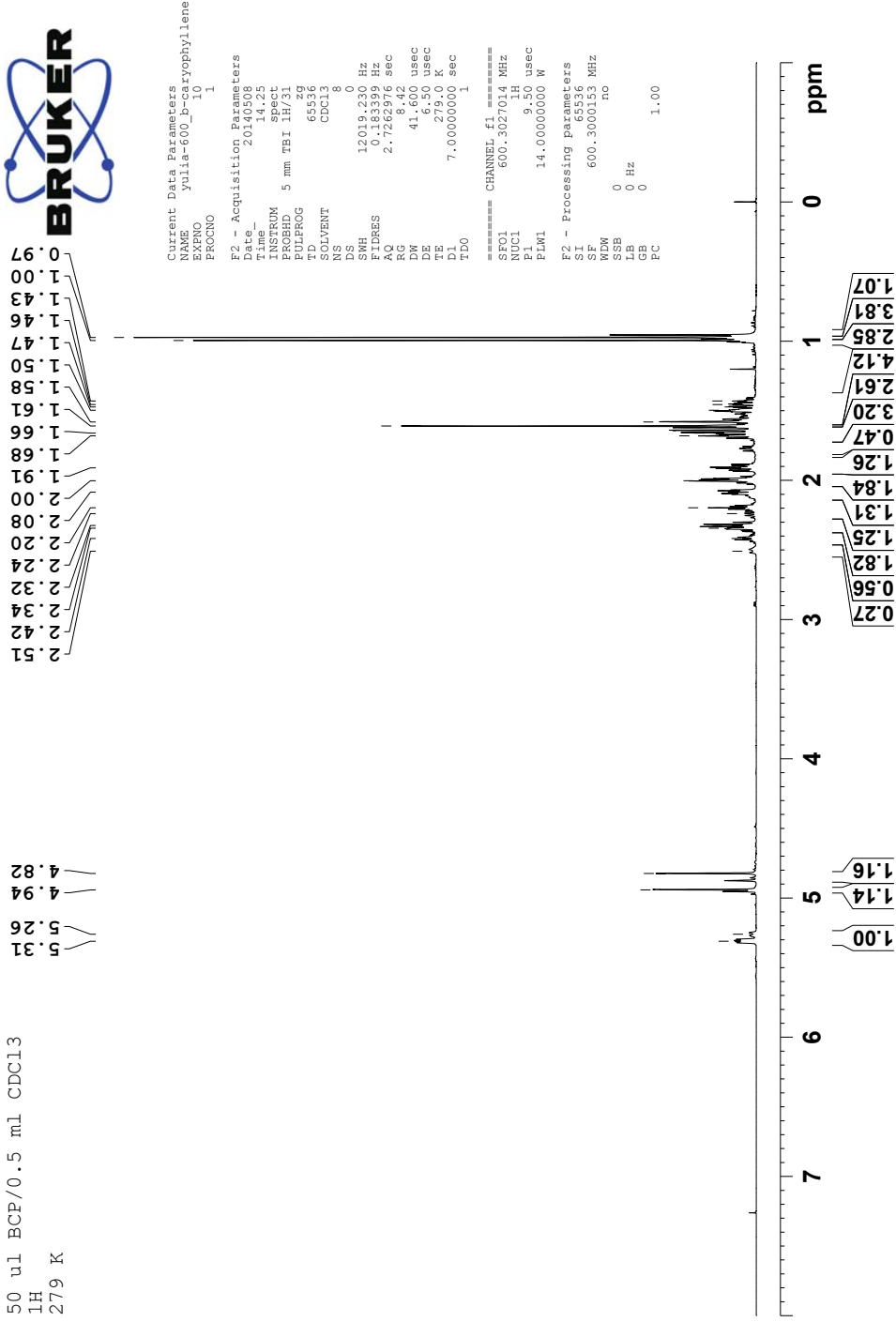
Note that our treatment of solvent quadrupolar splitting given by Eq. (1) is similar to others^[20], but introduces explicitly the probability of interaction between solvent and chains, given by the dilution factor ϕ in the equation, and identifies ε the efficiency for transfer of orientation. A more in-depth study of the validity of Eq. (1), and in particular on its dependence on the order parameter S of the monomers, is in principle possible by using a combination of deuterated solvents with non-deuterated chains, and deuterated chains with non-deuterated solvents. This might be crucial if, as we anticipate here, there are certain cases where ε might be S -dependent, for instance when the size of the solvent molecule is much larger than the size of the chain monomers, and the resulting interactions between the chain monomer and the solvent lose their local character.

Being able to quantitatively treat quadrupolar splitting in anisotropically swollen gels will not only provide an operational framework for dealing with orientation media in RDC experiments, but will also open a spectrum of new interesting possibilities to study the interactions of gels with different molecules. A particularly relevant example concerns gel swelling in solvent mixtures, say for the sake of clarity, in binary solvent mixtures. Since the value of quadrupolar splitting depends explicitly on the probability of encounter between a given solvent molecule and the chain monomers, the dependence of measured values of quadrupolar splitting $\Delta\nu_Q$ as a function of X , the molar ratio of one of the solvents in the mixture, should be very sensitive to phenomena akin to preferential solvation. Thus, we would expect a smooth linear interpolation between two values for $\Delta\nu_Q$ as a function of X if the two solvents are equally good for the polymer, while any preferential solvent character will increase its probability of contact with the chains above its average value, promoting markedly non-linear variations of $\Delta\nu_Q$ with X .

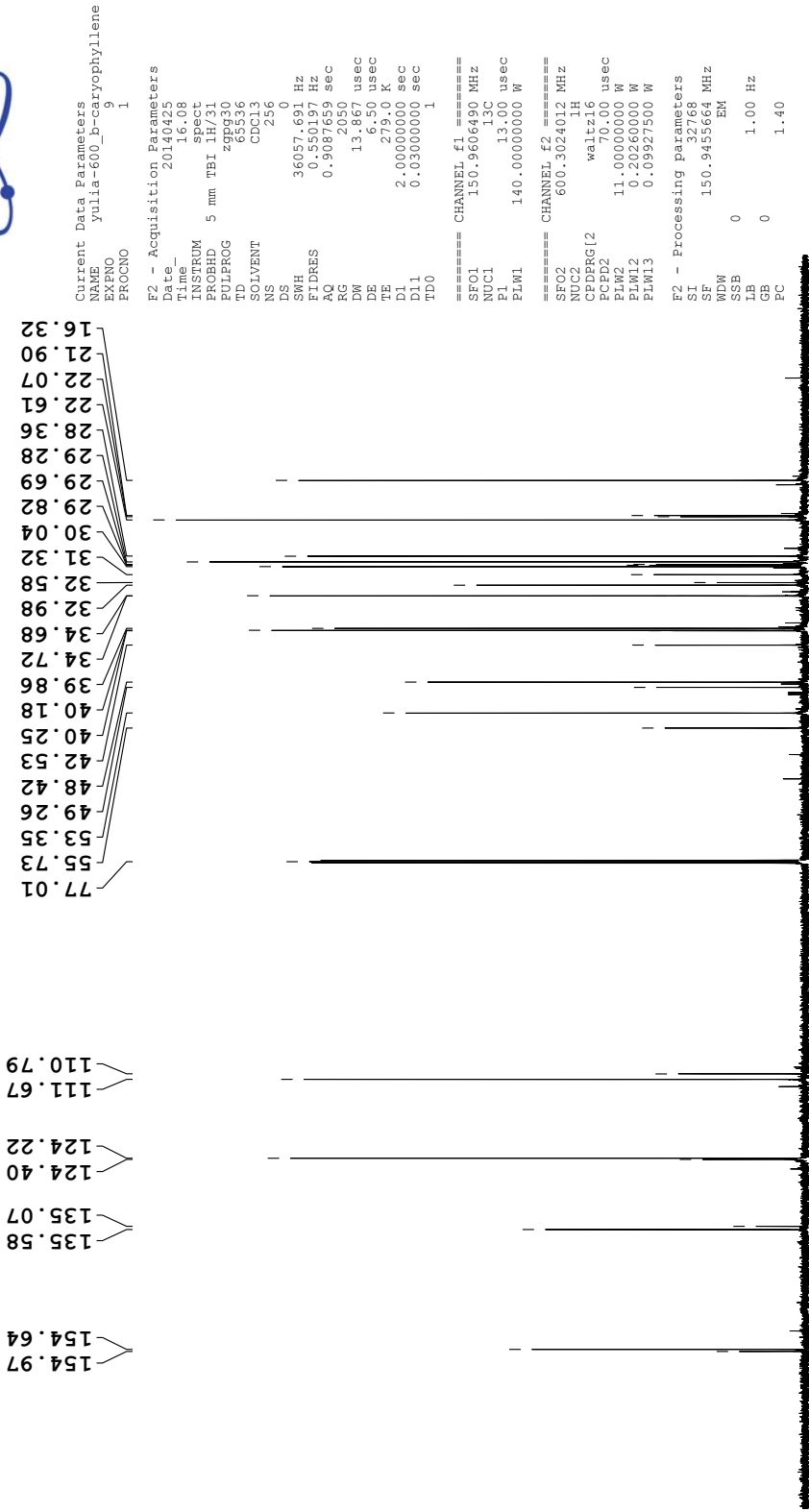
NMR spectra

¹H NMR of BCP/CDCl₃, 279 K

50 uL BCP/0.5 mL CDCl₃
¹H
 279 K

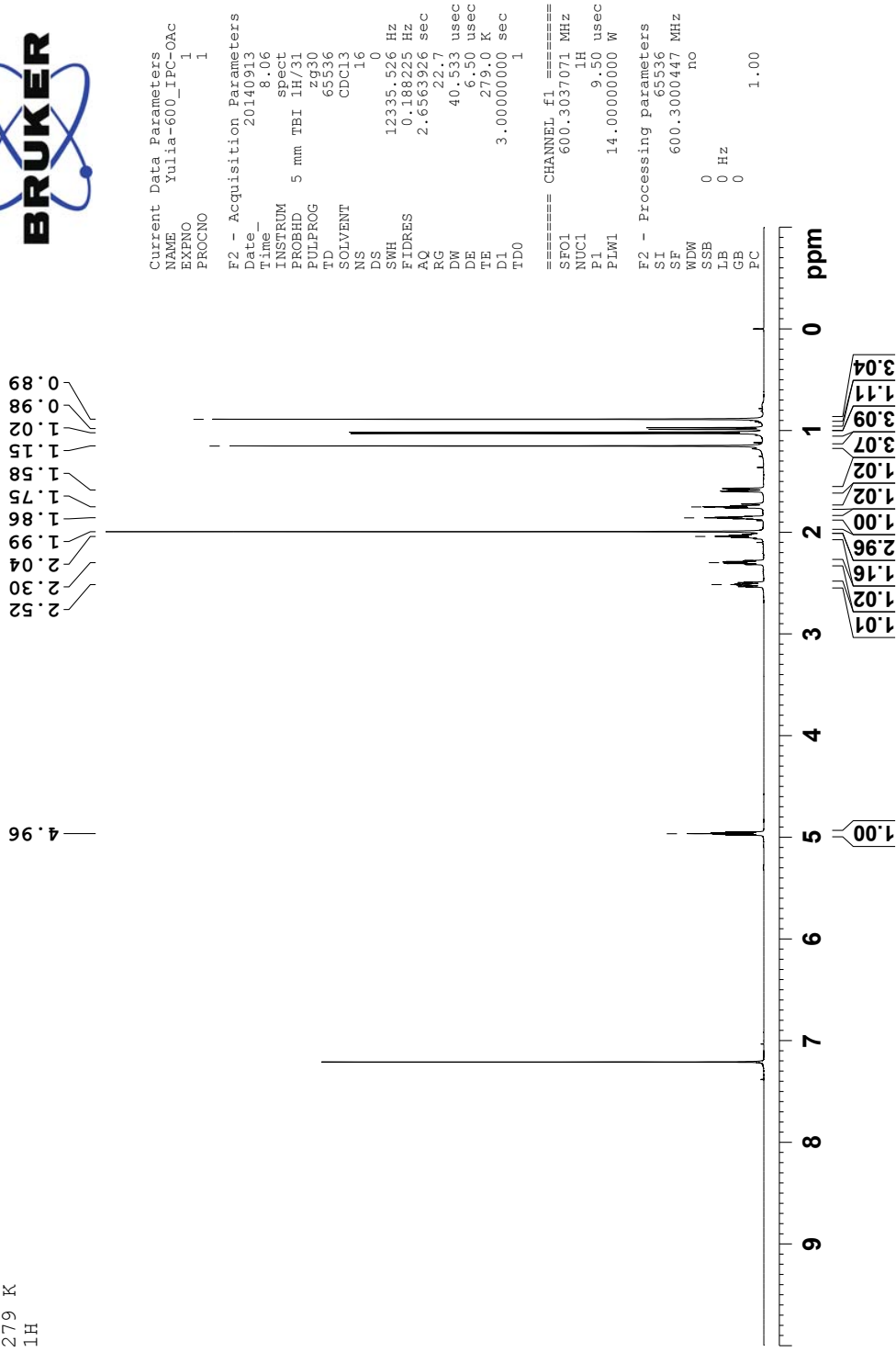


¹³C NMR of BCP/CDCl₃, 279 K
 50 µl BCP/ 0.5 ml CDCl₃
¹³C
 279 K

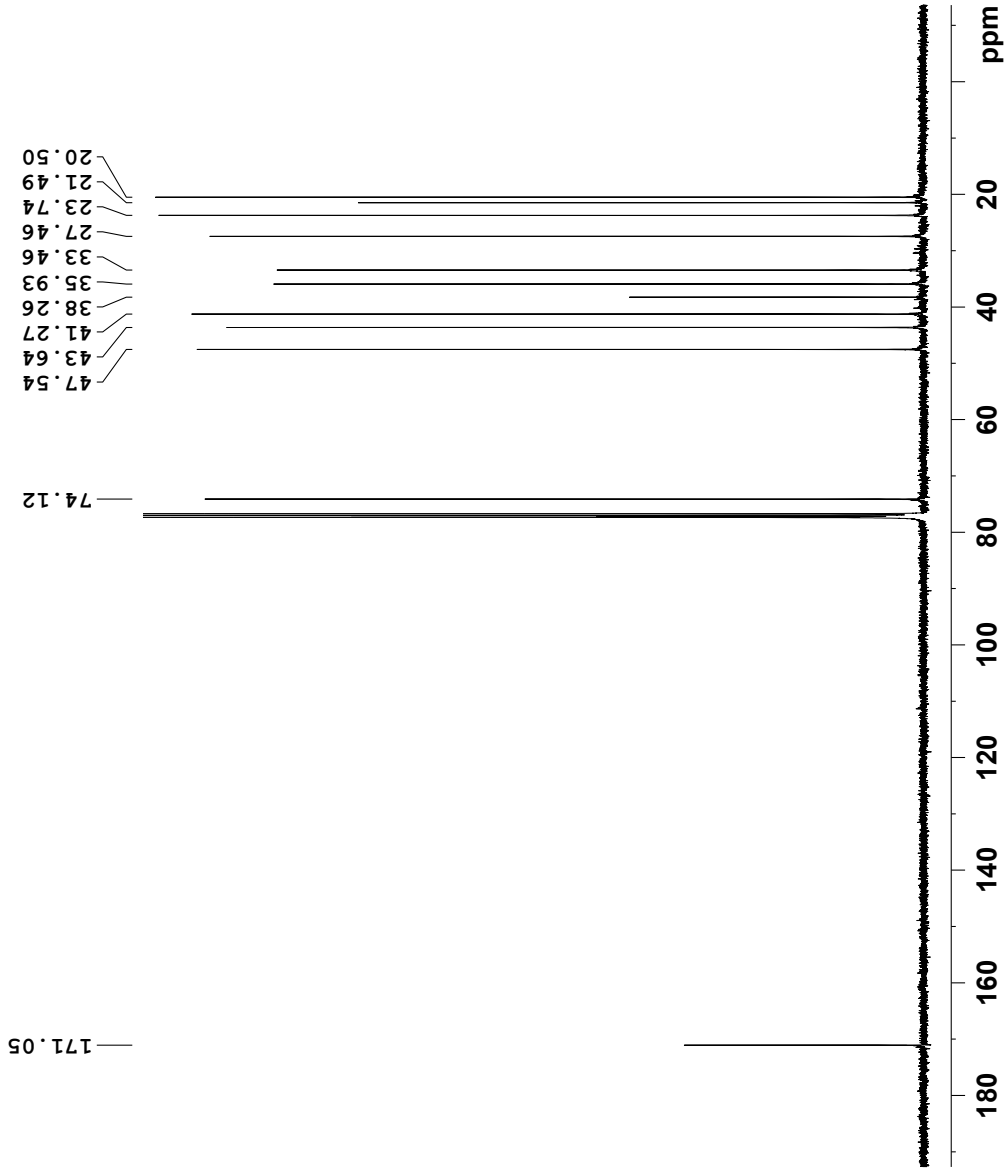


¹H NMR of (+)IPC-OAc/CDCl₃, 279 K

IPC-OAc in CDCl₃
279 K
1H



¹³C NMR of (+)IPC-OAc/CDCl₃, 279 K



```

Current Data Parameters
NAME      Yulia-600_IPC-OAc
EXPNO    2
PROCNO   1

F2 - Acquisition Parameters
Date_    20140909
Time     7.46
INSTRUM spect
PROBHD   5 mm PABBO BB/
PULPROG zgpg30
TD       65536
SOLVENT  CDCl3
NS       1024
DS       0
SWH      24038.461 Hz
FIDRES   0.366798 Hz
AQ       1.3631488 sec
RG       2050
DW       20.800 usec
DE       6.50 usec
TE       300.0 K
D1       2.00000000 sec
D11      0.03000000 sec
TD0      4

===== CHANNEL f1 =====
SFO1    100.6228293 MHz
NUC1    13C
P1      10.00 usec
PLW1    63.00000000 W

===== CHANNEL f2 =====
SFO2    400.1316005 MHz
NUC2    1H
PCPDZ   waitz16
PCPRG2  waitz16
PLW2    16.00000000 W
PLWI2   0.19750000 W
PLWI3   0.16000000 W

F2 - Processing parameters
SI       32768
SF       100.6127685 MHz
WDW      EM
SSB      0
LB       0
GB       0
PC       1.40
    
```

CLIP HSQC of BCP/CDCl₃, 279 K



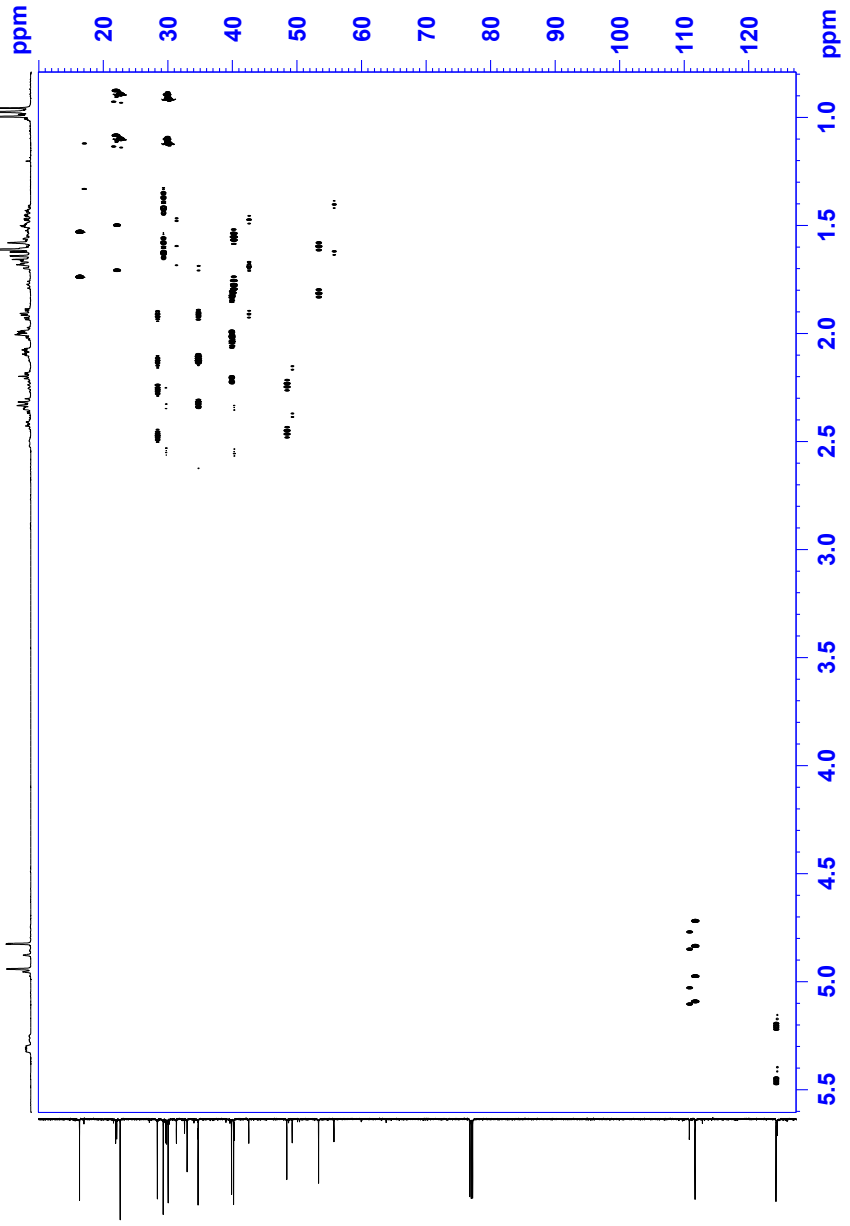
Current Data Parameters
 NAME yalia-600_f-cryophyllene
 PROCNO 1

F2 - Acquisition Parameters
 Date_ 20150116
 Time 11:15
 PROBHD 5 mm TBI 1H/1
 PULPROG hsqcetppp2
 SOLVENT CDCl₃
 NS 3
 DS 3
 SWH 7211.539 Hz
 FIDRES 0.289335 Hz
 AQ 1.440 sec
 DE 69.230 usec
 TE 300.2 K
 CHST2 165.8127940 K
 CD 1.00000000
 D1 1.50000000 sec
 D16 0.00327000 sec
 D17 0.00327000 sec
 INO 0.00002010 sec
 ZSOPFNS

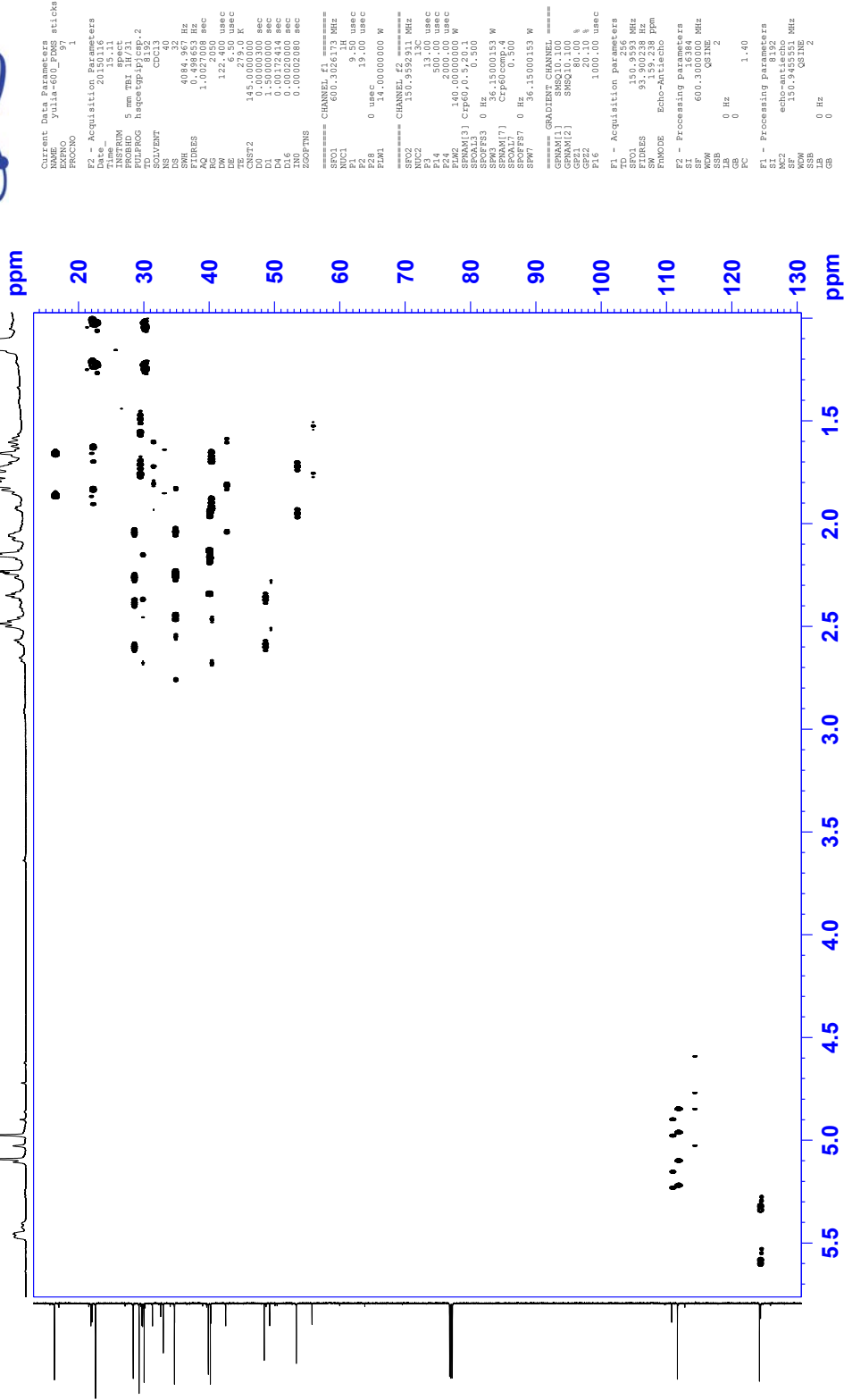
==== CHANNEL f1 =====
 NUC1 600.362411 MHz
 P1 9.50 usec
 P2 8 19.00 usec
 PLP1 14.00000000 W
 ===== CHANNEL f2 =====
 SF02 150.9561212 MHz
 P1C2 13.00 usec
 P14 300.00 usec
 PLW2 140.00000000 W
 SPMM(3) Cpf60,0.5,20.1
 SPOFFS3 0 Hz 0.500
 SPM3 36.15000153 W
 SPOA(7) Cpf60,0.5,20.1
 SPOA(7) 0.500
 SPOFFS7 0 Hz 36.15000153 W
 SPM7

==== GRADIENT CHANNEL =====
 GPCP1 80.00 %
 GPCP2 80.00 %
 GPCP3 80.00 %
 GPCP4 80.00 %
 GPCP5 100.00 usec
 GPCP6 100.00 usec
 TD 256
 SFO1 150.9561212 MHz
 FIDRES 0.289335 Hz
 SW 154.787 ppm
 ENMODE Echo-Antiecho

F2 - Processing parameters
 SI 6136 MHz
 WDW 600.300250 MHz
 SSB 0 Hz
 GB 0
 PC 1.40
 F1 - Processing parameters
 SI2 echo-ant,2048
 SF2 150.945551 MHz
 RDW 0 Hz
 LIB 0
 GB 0



CLIP HSQC of BCP/2.6% PDMS/CDCl₃, 279 K



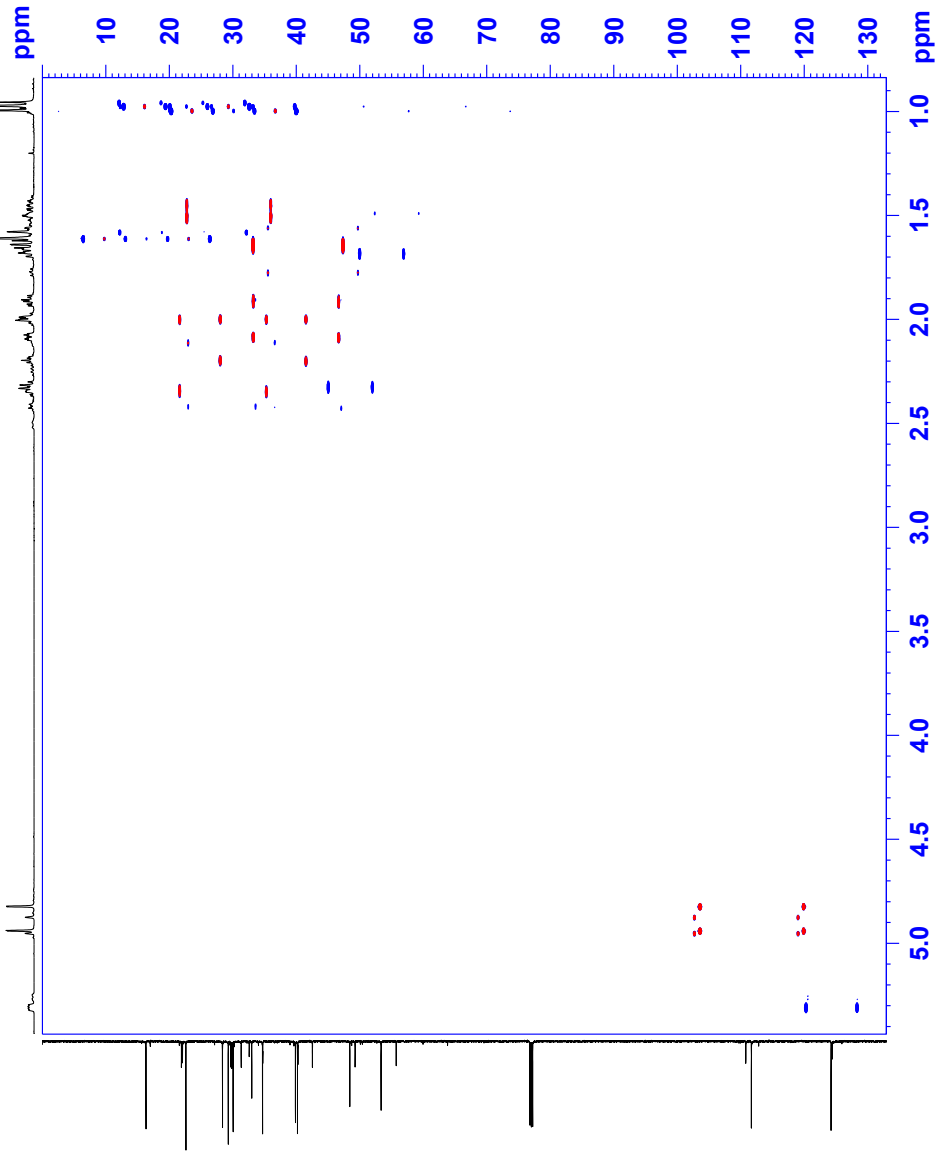
Current Data Parameters sticks
 EXNO yulia-60U_F01 1
 PROCNO 1
 F2 - Acquisition Parameters
 Date_ 20150116
 INSTRUM spect
 PULPROG zgpg30
 TD 65536
 SOLVENT CDCl3
 DS 32
 SWH 4084.867 Hz
 FIDRES 1.01274088 Hz
 AQ 1.01274088 sec
 RG 2050
 DE 12.650 usec
 TE 300.2 K
 CPDPRG2 145.000275.0 K
 DD 0.00000300 sec
 D1 1.50000000 sec
 D16 0.00020000 sec
 ZDELTA 0.00020000 sec
 ===== CHANNEL f1 =====
 NUC1 13C
 P1 13.00 usec
 PL1 0 dB
 ===== CHANNEL f2 =====
 NUC2 1H
 P2 13.00 usec
 PL2 0 dB
 ===== Acquisition Parameters =====
 F1 - Acquisition Parameters
 TD 65536
 FIDRES 93.900238 Hz
 SFO 150.943000 MHz
 SWH 159.238 Ppm
 FWHM 1.59238 Hz
 ===== Processing Parameters =====
 SF 600.300000 MHz
 GB 0 Hz
 LB 0 Hz
 GB 0
 PC 1.40
 ===== Processing Parameters =====
 SI echo-antlecho
 SC 150.943000 MHz
 SS 150.943000 MHz
 SSB 0 Hz
 CB 0

*F*₁-coupled HSQC (BIRD-filtered variant, scaling factor =8) of BCP/CDCl₃, 279 K



```

Current Data Parameters
EXPNO 3
PROCNO 1
F2 - Acquisition Parameters
Time 20.1453
INSTRUM spect
PULPROG hsqcblatp2f2p-2
TD 1200
AQ 0.00000000
RG 10
NS 10
DSB 4807.632 Hz
FIDRES 4.006410 Hz
RG 0.12480000 sec
DM 104.0000 usec
TE 279.2 K
CNS22 145.0000000
D0 0.00000000
D1 2.00000000 sec
D4 0.00172414 sec
D11 0.00000000 sec
D20 0.00000000 sec
IN20 0.00014724 sec
===== CHANNEL f1 =====
SFO1 600.3018009 MHz
NUC1 1H
P2 19.00 usec
PCPA 0 usec
===== CHANNEL f2 =====
SFO2 500.1307 MHz
NUC2 13C
PCPD12 13.00 usec
P14 500.00 usec
PCPD2 60.00 usec
PCPD3 60.00 usec
PCPD4 140.00000000 W
PCPD5 140.00000000 W
PCPD6 0.5, 20.1
SFO1L3 0 Hz
SFO2L3 36.15000153 M
SFO1M4 0 Hz
SFO2M4 0 Hz
SFO1F4 0 Hz
SFO2F4 59.15000153 M
===== GRADIENT CHANNEL =====
GPM1L1 0 Hz
GPM1L2 0 Hz
GPM1L3 0 Hz
GPM1L4 0 Hz
GPM2L1 0 Hz
GPM2L2 0 Hz
GPM2L3 0 Hz
GPM2L4 0 Hz
===== Acquisition parameters =====
SFO1 600.3018009 MHz
SFO2 500.1307 MHz
SM 1300.010 ppm
FWD02E Echo-Antiecho
F2 - Processing parameters
SI 600.30001024 MHz
RG 10
LB 0 Hz
GB 0 Hz
FC 1.40
F1 - Processing parameters
KC2 echo-antiecho
SF 150.9453551 MHz
SBR 0.3312
GB 0 Hz
  
```



*F*₁-coupled HSQC with MQ evolution of BCP/CDCl₃, 279 K



Current Data Parameters
 NAME yulia-60_h-capryphylene
 PROCNO 1

F2 - Acquisition Parameters
 Date_ 20131112
 INSTRUM spect
 INTPROG zgpg30
 F2PROG zgpg30

TD 65536
 CH1 12
 NS 12
 DS 4

SWH 4807.652 Hz
 FIDRES 4.006410 Hz
 AQ 1.166100 sec
 RG 1024
 DE 154.450 usec
 KE 6.50 usec

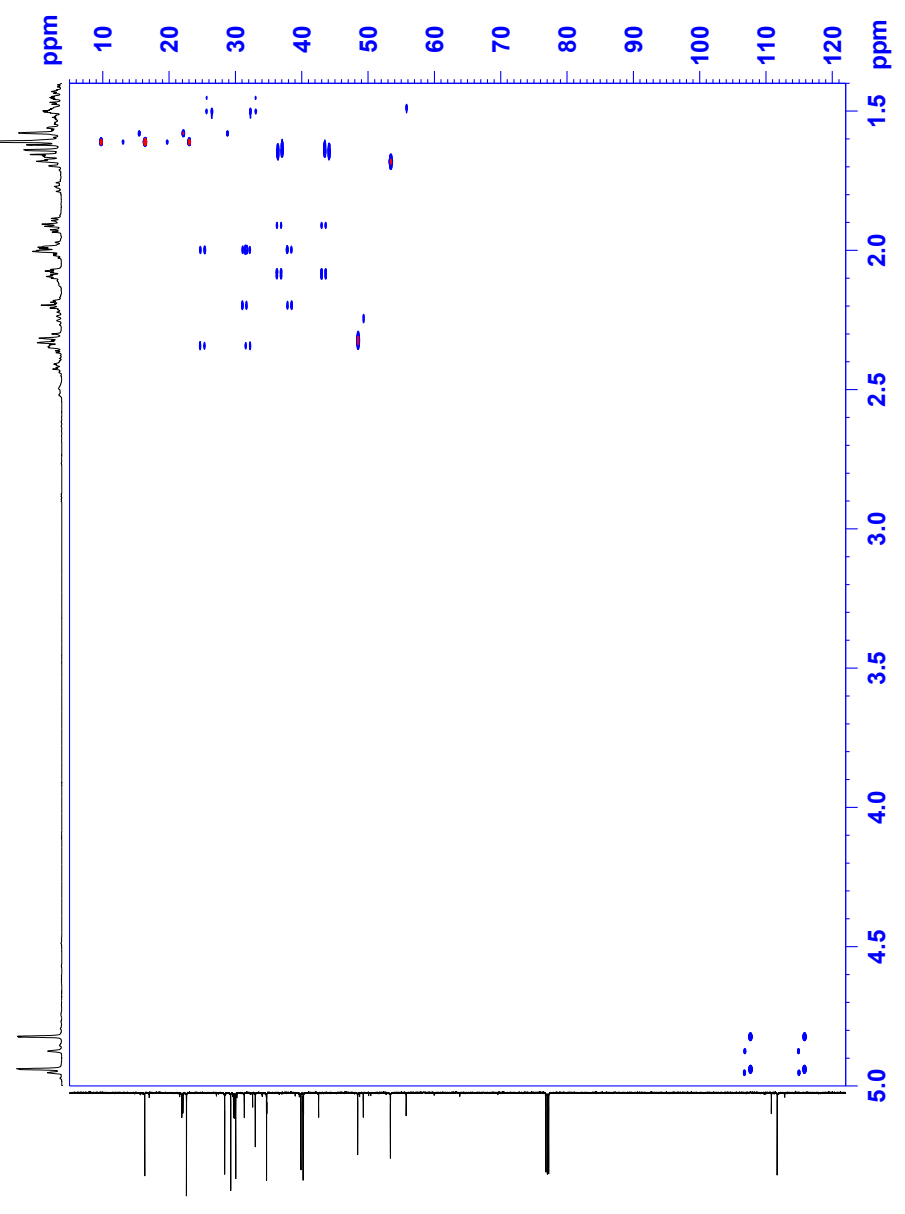
TE 300.2 K
 ZNUC2 145.007910 K
 ZNUC1 6.0000000 K

CHEM16 8.0000000
 CHEM17 0.0000000
 D0 0.0000000 usec
 D1 2.0000000 usec
 D2 2.0000000 usec
 D3 0.0017244 usec
 D4 0.0017244 usec
 D16 0.0020000 usec
 D30 0.0020000 usec
 D35 0.0018400 usec
 INE0 0.0014720 usec

===== CHANNEL f1 =====
 NUCL1 13C
 P1 9.50 usec
 PL1 14.0000000 W
 ===== CHANNEL f2 =====
 SR02 150.976307 MHz
 CPDPRG2 zgpg30
 P14 9.00 usec
 PL4 300.00 usec
 P2A 2000.00 usec
 PLAZ 140.0000000 W
 SFOAL2 0 Hz 0.500
 SFOAL3 C1F6D2.5281
 SFOAL4 150.976307 MHz
 SFOAL5 0 Hz 0.500
 SFOAL7 C1F6D2.5281
 SFOAL8 0 Hz 0.500
 SFOAL9 0 Hz
 SFOALF7 0 Hz
 SFOALF9 0 Hz 0.5000453 W

===== CHANNEL f3 =====
 CPDPRG31 SFG30
 GPRM11 SFG30.100
 GPRM12 SFG30.100
 GPRM13 SFG30.100
 GPRM14 SFG30.100
 GPRM15 SFG30.100
 GPRM16 SFG30.100
 GPRM17 SFG30.100
 GPRM18 SFG30.100
 GPRM19 SFG30.100
 GPRM20 SFG30.100
 GPRM21 SFG30.100
 GPRM22 SFG30.100
 GPRM23 SFG30.100
 GPRM24 SFG30.100
 GPRM25 SFG30.100
 GPRM26 SFG30.100
 GPRM27 SFG30.100
 GPRM28 SFG30.100
 GPRM29 SFG30.100
 GPRM30 SFG30.100
 GPRM31 SFG30.100
 GPRM32 SFG30.100
 GPRM33 SFG30.100
 GPRM34 SFG30.100
 GPRM35 SFG30.100
 GPRM36 SFG30.100
 GPRM37 SFG30.100
 GPRM38 SFG30.100
 GPRM39 SFG30.100
 GPRM40 SFG30.100
 GPRM41 SFG30.100
 GPRM42 SFG30.100
 GPRM43 SFG30.100
 GPRM44 SFG30.100
 GPRM45 SFG30.100
 GPRM46 SFG30.100
 GPRM47 SFG30.100
 GPRM48 SFG30.100
 GPRM49 SFG30.100
 GPRM50 SFG30.100

F1 - Acquisition Parameters
 TPO1 150.924 MHz
 FIDRES 26.337024 Hz
 AQC2 1.166100 sec
 RG 1024
 DE 154.450 usec
 KE 6.50 usec
 PWDIAP ECHO-DELTA
 F2 - Processing Parameters
 SI 1024
 MDW 600.30024 MHz
 SSB 0 Hz
 GB 0
 PC 1.40
 SI - Processing Parameters
 SFC2 echo-antisubs
 MDW 150.924 MHz
 SSB 0 Hz
 GB 0



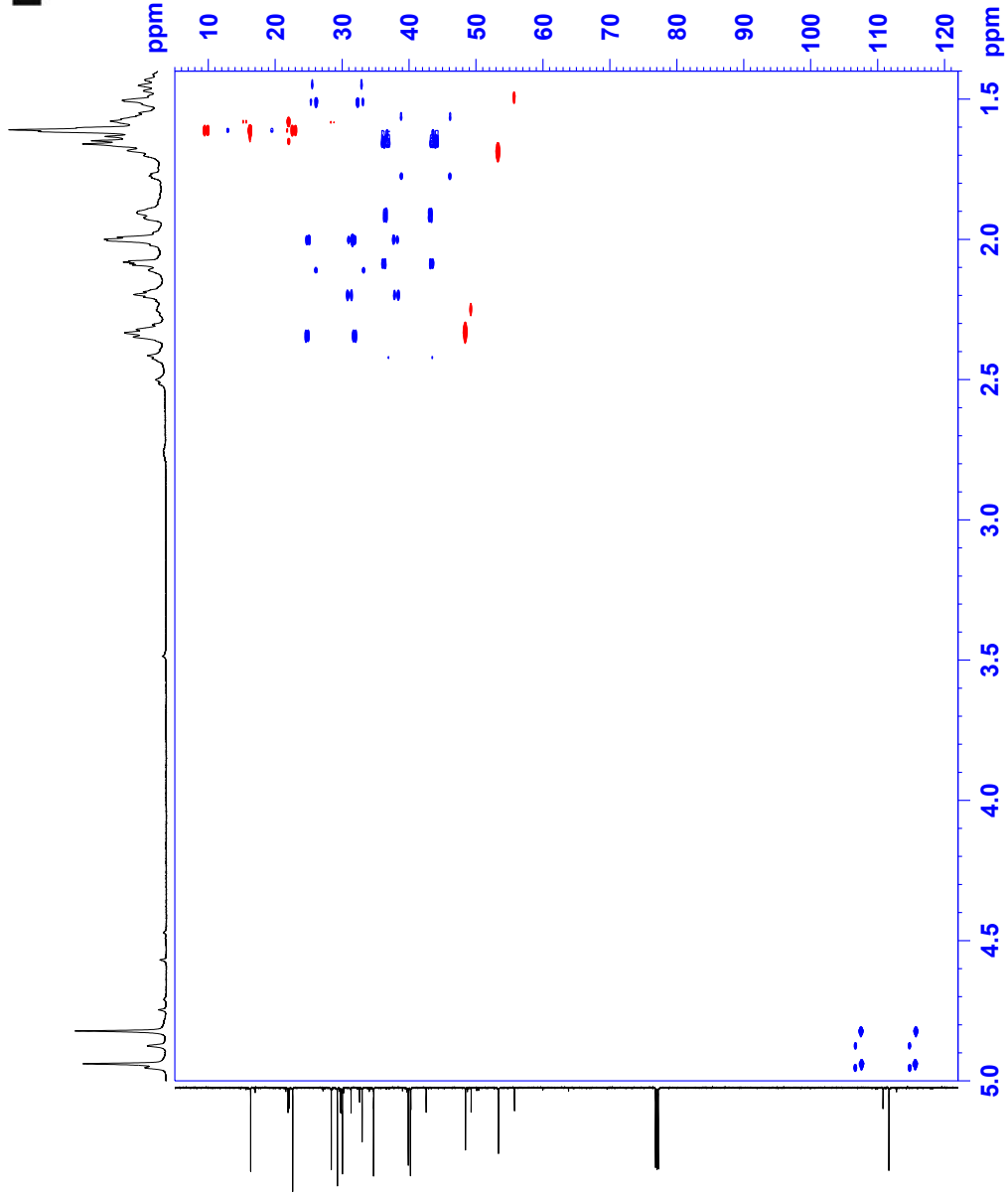
F₁-coupled HSQC with MQ evolution of BCP/2.6% PDMS/CDCl₃, 279 K



```

===== Data Parameters =====
NAME:      ymlia-600_Pdms atCl3
PROCNO:    1
===== Acquisition Parameters =====
Date_:     20141113
Time:      11:31:31
PROBHD:    5 mm TBI /1H/31
PULPROG:   zgpg30
TD:        65536
SFO:        600.1360000 MHz
WDW:        EM
SSB:        0
GB:         0
PC:         1.00
RG:         1024
AQ:         0.12249600 sec
RG2:        1024
RG3:         1024
RG4:         1024
RG5:         1024
RG6:         1024
RG7:         1024
RG8:         1024
RG9:         1024
RG10:       1024
RG11:       1024
RG12:       1024
RG13:       1024
RG14:       1024
RG15:       1024
RG16:       1024
RG17:       1024
RG18:       1024
RG19:       1024
RG20:       1024
RG21:       1024
RG22:       1024
RG23:       1024
RG24:       1024
RG25:       1024
RG26:       1024
RG27:       1024
RG28:       1024
RG29:       1024
RG30:       1024
RG31:       1024
RG32:       1024
RG33:       1024
RG34:       1024
RG35:       1024
RG36:       1024
RG37:       1024
RG38:       1024
RG39:       1024
RG40:       1024
RG41:       1024
RG42:       1024
RG43:       1024
RG44:       1024
RG45:       1024
RG46:       1024
RG47:       1024
RG48:       1024
RG49:       1024
RG50:       1024
RG51:       1024
RG52:       1024
RG53:       1024
RG54:       1024
RG55:       1024
RG56:       1024
RG57:       1024
RG58:       1024
RG59:       1024
RG60:       1024
RG61:       1024
RG62:       1024
RG63:       1024
RG64:       1024
RG65:       1024
RG66:       1024
RG67:       1024
RG68:       1024
RG69:       1024
RG70:       1024
RG71:       1024
RG72:       1024
RG73:       1024
RG74:       1024
RG75:       1024
RG76:       1024
RG77:       1024
RG78:       1024
RG79:       1024
RG80:       1024
RG81:       1024
RG82:       1024
RG83:       1024
RG84:       1024
RG85:       1024
RG86:       1024
RG87:       1024
RG88:       1024
RG89:       1024
RG90:       1024
RG91:       1024
RG92:       1024
RG93:       1024
RG94:       1024
RG95:       1024
RG96:       1024
RG97:       1024
RG98:       1024
RG99:       1024
RG100:      1024
===== Processing parameters =====
SI:         32768
SF:         600.1360000 MHz
WDW:        EM
SSB:        0
GB:         0
PC:         1.00
===== Channel f1 =====
SFO1:       600.1360000 MHz
NUC1:       13C
P1:         12.00 usec
PL1:        0.00 dB
SFO2:       125.7613300 MHz
NUC2:       1H
P2:         12.00 usec
PL2:        0.00 dB
===== Channel f2 =====
SFO:        600.1360000 MHz
NUC:        13C
P:          12.00 usec
PL:         0.00 dB
===== Acquisition parameters =====
SFO:        600.1360000 MHz
WDW:        EM
SSB:        0
GB:         0
PC:         1.00
===== Processing parameters =====
SI:         32768
SF:         600.1360000 MHz
WDW:        EM
SSB:        0
GB:         0

```



CLIP HSQC of IPC-OAc/ CDCl_3 , 279 K



Current Pulse Parameters
 NAME vllla-600_ipc-oac
 EXPMO 4
 PROCNO 1

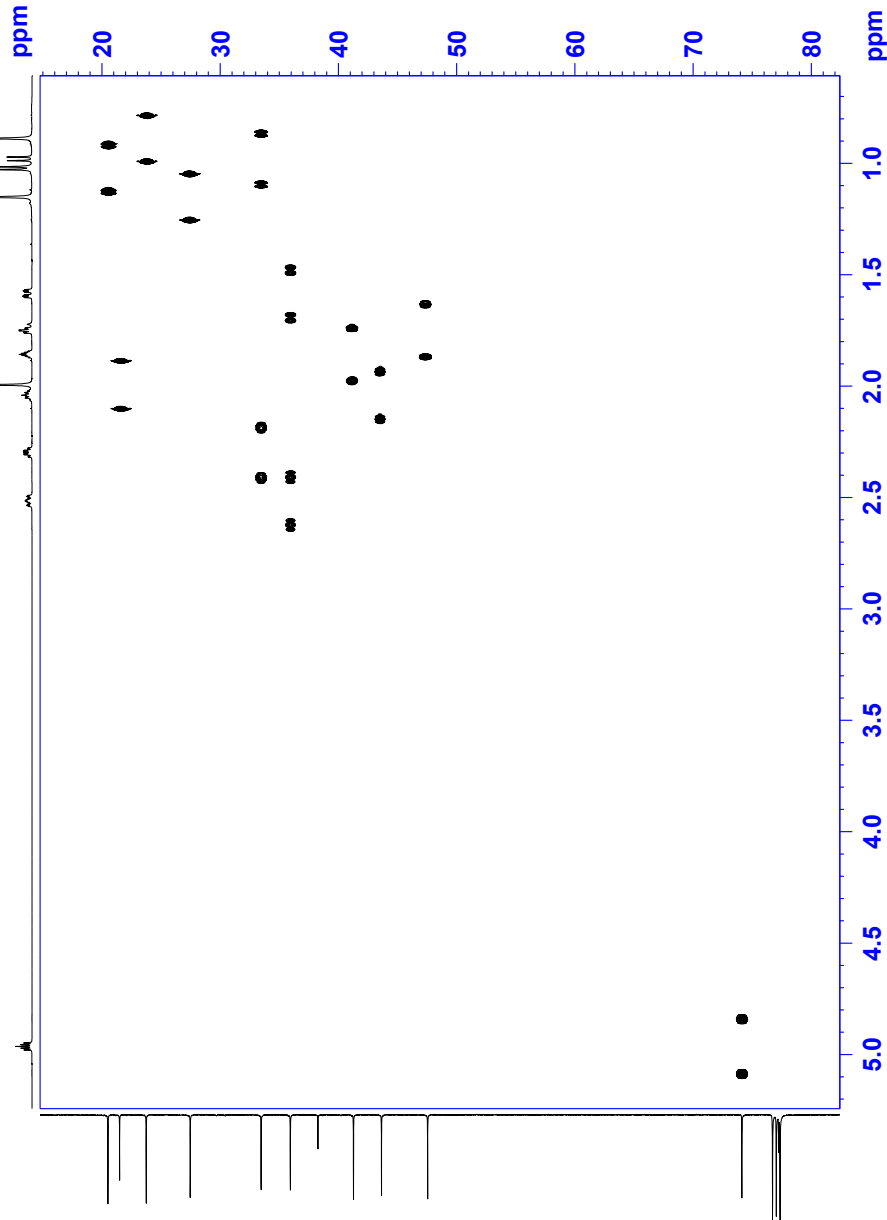
F2 - Acquisition Parameters
 Date_ 2015.10.03
 Time 19.03
 INSTRUM spect
 PULPROG zgpg30
 F2PROC zgpg30
 TD 8192
 SFO 600.132
 NS 2048
 DS 4
 SWH 600.32
 FIDRES 0.731696
 AQ 0.681744
 SFO2 600.132
 DWDW 83.200
 DE 6.50
 CHST2 145.000000
 DD 0.000000
 D4 0.000000
 D16 0.000000
 ZDELTA 0.000000
 ZDELTA2 0.000000

===== CHANNEL f1 =====
 SFO1 400.1424012
 NUC1 1H
 P1 9.00
 F2 39.00
 PLW1 14.00000000
 SFO2 150.9561312
 P2 13.00
 PLW2 200.00
 SFO3 140.00000000
 SFOFF3 0
 SFO4 26.13000153
 SFOFF4 0
 SFO5 36.13000153
 SFOFF5 0
 SFO6 56.15000153
 SFOFF6 0

===== GRADIENT CHANNEL =====
 GPC1 80.00
 GPC2 80.00
 GPC3 80.00
 GPC4 80.00
 GPC5 80.00
 GPC6 80.00
 GPC7 80.00
 GPC8 80.00
 GPC9 80.00
 GPC10 80.00
 GPC11 80.00
 GPC12 80.00
 GPC13 80.00
 GPC14 80.00
 GPC15 80.00
 GPC16 80.00
 GPC17 80.00
 GPC18 80.00
 GPC19 80.00
 GPC20 80.00
 GPC21 80.00
 GPC22 80.00
 GPC23 80.00
 GPC24 80.00
 GPC25 80.00
 GPC26 80.00
 GPC27 80.00
 GPC28 80.00
 GPC29 80.00
 GPC30 80.00
 GPC31 80.00
 GPC32 80.00
 GPC33 80.00
 GPC34 80.00
 GPC35 80.00
 GPC36 80.00
 GPC37 80.00
 GPC38 80.00
 GPC39 80.00
 GPC40 80.00
 GPC41 80.00
 GPC42 80.00
 GPC43 80.00
 GPC44 80.00
 GPC45 80.00
 GPC46 80.00
 GPC47 80.00
 GPC48 80.00
 GPC49 80.00
 GPC50 80.00
 GPC51 80.00
 GPC52 80.00
 GPC53 80.00
 GPC54 80.00
 GPC55 80.00
 GPC56 80.00
 GPC57 80.00
 GPC58 80.00
 GPC59 80.00
 GPC60 80.00
 GPC61 80.00
 GPC62 80.00
 GPC63 80.00
 GPC64 80.00
 GPC65 80.00
 GPC66 80.00
 GPC67 80.00
 GPC68 80.00
 GPC69 80.00
 GPC70 80.00
 GPC71 80.00
 GPC72 80.00
 GPC73 80.00
 GPC74 80.00
 GPC75 80.00
 GPC76 80.00
 GPC77 80.00
 GPC78 80.00
 GPC79 80.00
 GPC80 80.00
 GPC81 80.00
 GPC82 80.00
 GPC83 80.00
 GPC84 80.00
 GPC85 80.00
 GPC86 80.00
 GPC87 80.00
 GPC88 80.00
 GPC89 80.00
 GPC90 80.00
 GPC91 80.00
 GPC92 80.00
 GPC93 80.00
 GPC94 80.00
 GPC95 80.00
 GPC96 80.00
 GPC97 80.00
 GPC98 80.00
 GPC99 80.00
 GPC100 80.00

F1 - Acquisition Parameters
 TD 256
 SFO1 150.9561
 SFO2 150.9561
 SFO3 150.9561
 SFO4 150.9561
 SFO5 150.9561
 SFO6 150.9561
 SFO7 150.9561
 SFO8 150.9561
 SFO9 150.9561
 SFO10 150.9561
 SFO11 150.9561
 SFO12 150.9561
 SFO13 150.9561
 SFO14 150.9561
 SFO15 150.9561
 SFO16 150.9561
 SFO17 150.9561
 SFO18 150.9561
 SFO19 150.9561
 SFO20 150.9561
 SFO21 150.9561
 SFO22 150.9561
 SFO23 150.9561
 SFO24 150.9561
 SFO25 150.9561
 SFO26 150.9561
 SFO27 150.9561
 SFO28 150.9561
 SFO29 150.9561
 SFO30 150.9561
 SFO31 150.9561
 SFO32 150.9561
 SFO33 150.9561
 SFO34 150.9561
 SFO35 150.9561
 SFO36 150.9561
 SFO37 150.9561
 SFO38 150.9561
 SFO39 150.9561
 SFO40 150.9561
 SFO41 150.9561
 SFO42 150.9561
 SFO43 150.9561
 SFO44 150.9561
 SFO45 150.9561
 SFO46 150.9561
 SFO47 150.9561
 SFO48 150.9561
 SFO49 150.9561
 SFO50 150.9561
 SFO51 150.9561
 SFO52 150.9561
 SFO53 150.9561
 SFO54 150.9561
 SFO55 150.9561
 SFO56 150.9561
 SFO57 150.9561
 SFO58 150.9561
 SFO59 150.9561
 SFO60 150.9561
 SFO61 150.9561
 SFO62 150.9561
 SFO63 150.9561
 SFO64 150.9561
 SFO65 150.9561
 SFO66 150.9561
 SFO67 150.9561
 SFO68 150.9561
 SFO69 150.9561
 SFO70 150.9561
 SFO71 150.9561
 SFO72 150.9561
 SFO73 150.9561
 SFO74 150.9561
 SFO75 150.9561
 SFO76 150.9561
 SFO77 150.9561
 SFO78 150.9561
 SFO79 150.9561
 SFO80 150.9561
 SFO81 150.9561
 SFO82 150.9561
 SFO83 150.9561
 SFO84 150.9561
 SFO85 150.9561
 SFO86 150.9561
 SFO87 150.9561
 SFO88 150.9561
 SFO89 150.9561
 SFO90 150.9561
 SFO91 150.9561
 SFO92 150.9561
 SFO93 150.9561
 SFO94 150.9561
 SFO95 150.9561
 SFO96 150.9561
 SFO97 150.9561
 SFO98 150.9561
 SFO99 150.9561
 SFO100 150.9561

F1 - Processing parameters
 SI 4096
 SF 150.945551
 WDW 0
 SSB 0
 GB 0
 PC 1.40

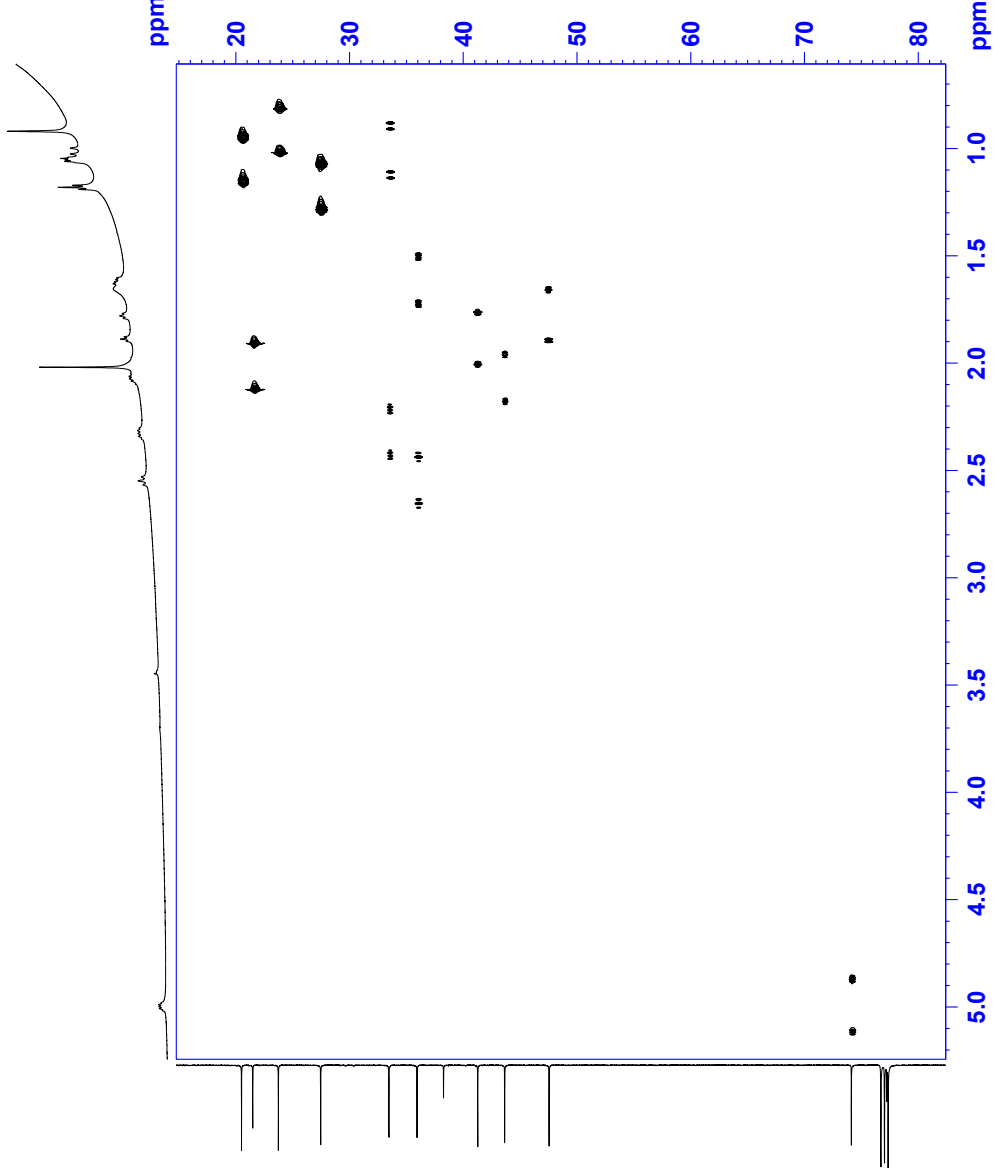


CLIP HSQC of IPC-OAc / 2.6% PDMS/CDCl₃, 279 K



```

Current Data Parameters
EXPNO 8
PROCNO 1
F2 - Acquisition Parameters
Date_ 20140914
Time 17:11
INSTRUM spect
PROBHD 5 mm TBI 1H/13
PULPROG hsqcgppp1p2
TD 65536
FIDRES 0.192
SOLVENT CDCl3
DS 32
SWH 609.615 Hz
F2 - F1 150.913 MHz
AQ 0.613744 sec
RG 2050
AQ 0.613744 sec
DD 6.50 usec
TE 279.0 K
DS2 145.000000 sec
DD2 0.000000 sec
D1 1.5000000 sec
d11 0.0000000 sec
D2 0.0000000 sec
D3 0.0020000 sec
D6 0.0020000 sec
IND 0.0000010 sec
ZOGPINS
===== CHANNEL f1 =====
NUC1 13
NUC2 1H
P1 9.50 usec
P2 0 usec
P3 19.00 usec
PL1 14.0000000 W
===== CHANNEL f2 =====
SF02 150.9561212 MHz
NUC2 13
P2 13.00 usec
P3 500.00 usec
P4 2000.00 usec
P5 2000.00 usec
P6 2000.00 usec
SFO2 140.0000000 MHz
SFO3 0 Hz
SFO4 0.500
SFO5 36.15000153 W
SFO6 Crp6comp.4
SFO7 0 Hz
SFO8 0.500
SFO9 36.15000153 W
===== GRADIENT CHANNEL =====
GDMAX1 88.0000000 MHz
GDMAX2 88.0000000 MHz
GFE1 20.10 %
GFE2 20.10 %
P6 1000.00 usec
F1 - Acquisition Parameters
SFO1 150.9561199 MHz
F2 - F1 150.913 MHz
FIDRES 0.192
PULPROG hsqcgppp1p2
PRGNAME Echo-Attacho
===== Processing parameters =====
SF 600.3001199 MHz
SFO1 150.9561199 MHz
SSB 0 Hz
LB 0 Hz
GB 0 Hz
PC 1.40
F1 - Processing parameters
SI 4096
MC2 echo-attacho
WFL 150.9561199 MHz
PRGNAME Echo-Attacho
SSB 0 Hz
LB 0 Hz
GB 0 Hz
  
```



References and Notes

- ¹ N.T. Nyberg, J.Ø. Duus, O.W. Sørensen, *J. Am. Chem. Soc.* 2005, **127**, 6154.
- ² a) D. H. Wu, A. Chen, C. S. Johnson, *J. Magn. Reson. Ser. A* 1995, **115**, 260; b) M. D. Pelta, H. Barjat, G. A. Morris, A. L. Davis, S. J. Hammond, *Magn. Res. Chem.* 1998, **36**, 706.
- ³ A. Enthart, J. C. Freudenberger, J. Furrer, H. Kessler, B. Luy, *J. Magn. Reson.* 2008, **192**, 314.
- ⁴ a) K. Fehér, S. Berger, K. E. Kövér, *J. Magn. Reson.* 2003, **163**, 340; b) C. M. Thiele, W. Bermel, *J. Magn. Reson.* 2012, **216**, 134.
- ⁵ K. E. Kövér, K. Fehér, *J. Magn. Reson.* 2004, **168**, 307.
- ⁶ L. Verdier, P. Sakhaii, M. Zweckstetter, C. Griesinger, *J. Magn. Reson.*, 2003, **163**, 353.
- ⁷ M. Hübner, B. Rissom and L. Fitjer, *Helv. Chim. Acta*, 1997, **80**, 1972.
- ⁸ M. Clericuzio, G. Alagona, C. Ghio and L. Toma, *J. Org. Chem.*, 2000, **65**, 6910.
- ⁹ F. Neese, *Wiley Interdiscip. Rev.: Comput. Mol. Sci.*, 2012, **2**, 73-78.
- ¹⁰ a) A. Krupp, PhD thesis, Technische Universität Darmstadt, Darmstadt, 2015. b) S. Immel, Technische Universität Darmstadt, Darmstadt, personal communication.
- ¹¹ F. Weigend and R. Ahlrichs, *Phys. Chem. Chem. Phys.*, 2005, **7**, 3297-3305.
- ¹² P. Trigo-Mouriño, C. Merle, M. R. M. Koos, B. Luy, R. R. Gil, *Chem. Eur. J.* 2013, **19**, 7013.
- ¹³ a) J. C. Freudenberger, P. Spiteller, R. Bauer, H. Kessler, B. Luy, *J. Am. Chem. Soc.*, 2004, **126**, 14690; b) J. Klages, C. Neubauer, M. Coles, H. Kessler, B. Luy, *Chembiochem*, 2005, **6**, 1672; c) P. Tzvetkova, S. Simova, B. Luy, *J. Magn. Res.*, 2007, **186**, 193; d) M. U. Kiran, A. Sudhakar, J. Klages, G. Kummerlowe, B. Luy, B. Jagadeesh, *J. Am. Chem. Soc.*, 2009, **131**, 15590; e) C. Gayathri, M. C. de la Fuente, B. Luy, R. R. Gil, A. Navarro-Vazquez, *Chem. Commun.*, 2010, **46**, 5879; f) G. Kummerlowe, E. F. McCord, S. F. Cheatham, S. Niss, R. W. Schnell, B. Luy, *Chem.-Eur. J.*, 2010, **16**, 7087; g) P. Tzvetkova, B. Luy, S. Simova, *Magn. Res. Chem.*, 2012, **50**, S92; h) S. Weigelt, T. Huber, F. Hofmann, M. Jost, M. Ritzefeld, B. Luy, C. Freudenberger, Z. Majer, E. Vass, J. C. Greie, L. Panella, B. Kaptein, Q. B. Broxterman, H. Kessler, K. Altendorf, M. Hollosi, N. Sewald, *Chem.-Eur. J.*, 2012, **18**, 478; i) G. Kummerlöwe, B. Luy, *Annu. Rep. NMR Spectrosc.*, 2009, **68**, 193; j) G. Kummerlöwe, S. Schmitt, B. Luy, *The Open Spectrosc. J.*, 2010, **4**, 16; k) L.-G. Xie, V. Bagutski, D. Audisio, L. Wolf, V. Schmidts, K. Hofmann, C. Wirtz, W. Thiel, C. M. Thiele, N. Maulide, *Chem. Sci.* **2015**, **6**, 5734-5739.
- ¹⁴ a) J.N. Lee, C. Park, G.M. Whitesides, *Anal. Chem.*, 2003, **75**, 6544; b) K.-S. Koh, J. Chin, J. Chia, C.-L. Chiang, *Macromachines*, 2012, **3**, 427.
- ¹⁵ E.J. Cabrita, S. Berger, *Magn. Reson. Chem.*, 2001, **39**, S142.
- ¹⁶ B. Deloche, A. Dubault, D. Durand, *J. Polymer Sci. B: Polymer Phys.*, 1992, **30**, 1419.
- ¹⁷ J.-U. Sommer and K. Saalwächter, *Macromol. Symp.*, 2010, **291-292**, 251.
- ¹⁸ P. J. Flory and J. Rehner, *J. Chem. Phys.*, 1943, **11**, 521.
- ¹⁹ P.G. de Gennes, *Scaling Concepts in Polymer Physics*, 1979, Cornell University Press.
- ²⁰ B. Deloche and E.T. Samulski, *Macromolecules*, 1981, **14**, 575.